Some Aspects of the Theory and Measurement of Frequency Fluctuations in Frequency Standards

L. S. CUTLER, MEMBER, IEEE, AND C. L. SEARLE, MEMBER, IEEE

Abstract—Precision quartz oscillators have three main sources of noise contributing to frequency fluctuations: thermal noise in the oscillator, additive noise contributed by auxiliary circuitry such as AGC, etc., and fluctuations in the quartz frequency itself as well as in the reactive elements associated with the crystal, leading to an f^{-1} type of power spectral density in frequency fluctuations. Masers are influenced by the first two types of noise, and probably also by the third.

The influence of these sources of noise on frequency fluctuation vs. averaging time measurements is discussed. The f^{-1}-spectral density leads to results that depend on the length of time over which the measurements are made. An analysis of the effects of finite observation time is given.

The characteristics of both passive and active atomic standards using a servo-controlled oscillator are discussed. The choice of servo time constant influences the frequency fluctuations observed as a function of averaging time and should be chosen for best performance with a given quartz oscillator and atomic reference.

The conventional methods of handling random signals, i.e., variances, autocorrelation, and spectral densities, are applied to the special case of frequency and phase fluctuations in oscillators, in order to obtain meaningful criteria for specifying oscillator frequency stability. The interrelations between these specifications are developed in the course of the paper.

I. Introduction

THE PURPOSE of this paper is to present some of the theoretical and practical aspects of frequency fluctuation measurements in frequency standards. In Section II the fundamental definitions of terms used in specifying frequency stability both in the time domain and the frequency domain are developed, and the interrelations between these terms are established. Section III describes briefly several of the commonly used techniques for measuring frequency stability and in each case relates the measurement to the appropriate mathematical description in Section II.

The three main sources of frequency fluctuation in oscillators are discussed in Section IV: thermal and shot noise in the oscillator, additive noise (in the amplifier, for example), and oscillator parameter changes giving rise to an f^{-1} power spectral density of frequency fluctuations. Finally, in Section V we consider the frequency fluctuations in atomic frequency standards.

Manuscript received October 11, 1965; revised December 1, 1965. This work was supported in part by the Joint Services Electronics Program under Contract DA-36-039-AMC-03200(E).

L. S. Cutler is with the Physics Research Division, Hewlett-Packard Company, Palo Alto, Calif.

C. L. Searle is with the Department of Electrical Engineering and the Research Laboratory of Electronics, Massachusetts Institute of Technology, Cambridge, Mass.

II. Specification of Frequency Stability

A. Definitions

The signal from an oscillator may be described by

$$v(t) = A(t) \cos [\omega_0 t + \phi(t)] \tag{1}$$

where $v(t)$ represents a voltage or current, $A(t)$ and $\phi(t)$ are slowly varying real functions of time, and ω_0 is a constant. $A(t)$ is the variable amplitude of the signal and does not contribute directly to frequency fluctuations. (Of course, in frequency multipliers and other nonlinear devices, conversion of amplitude modulation to phase modulation and vice versa can occur. Nonetheless, at any given point in the system, (1) is valid.) It is assumed that the time origin and ω_0 are chosen so that $\phi(t)$ has zero time average and

$$\lim_{T\to\infty} \frac{\phi(T/2) - \phi(-T/2)}{T} = 0.$$

These conditions simplify the mathematics (but will have to be relaxed later). The instantaneous angular frequency is

$$\omega(t) = \frac{d}{dt}[\omega_0 t + \phi(t)] = \omega_0 + \dot{\phi}(t). \tag{2}$$

In all that follows we will refer to angular frequency as frequency.

The average frequency of the signal $v(t)$ is by definition

$$\langle \omega(t) \rangle = \lim_{T\to\infty} \frac{1}{T} \int_{-T/2}^{T/2} \omega(t)\, dt$$

$$= \omega_0 + \lim_{T\to\infty} \frac{\phi(T/2) - \phi(-T/2)}{T} = \omega_0 \tag{3}$$

where the symbol $\langle\ \rangle$ indicates time average over an infinite time. Therefore, we see from (1) and (2) that $\phi(t)$ is the instantaneous phase angle of the oscillator with respect to an ideal oscillator of frequency ω_0, and $\dot{\phi}(t)$ is the frequency departure away from ω_0.

Of particular importance in the specification of frequency stability is the frequency departure averaged over some finite time τ:

Reprinted from *Proc. IEEE*, vol. 54, pp. 136–154, Feb. 1966.

$$\langle \dot{\phi} \rangle_{t,\tau} = \frac{1}{\tau} \int_{t-\tau/2}^{t+\tau/2} \dot{\phi}(t')\, dt' \tag{4a}$$

$$= \frac{\phi(t+\tau/2) - \phi(t-\tau/2)}{\tau} \tag{4b}$$

where the symbol $\langle\ \rangle_{t,\tau}$ signifies the average over a finite time τ, centered at time t. Similarly, we can define the finite-time average of the phase

$$\langle \phi \rangle_{t,\tau} = \frac{1}{\tau} \int_{t-\tau/2}^{t+\tau/2} \phi(t')\, dt'. \tag{5}$$

For future calculations we shall need the accumulated phase over a time τ. From (4),

$$\Delta_\tau \phi(t) \equiv \phi(t+\tau/2) - \phi(t-\tau/2) = \tau \langle \dot{\phi} \rangle_{t,\tau}. \tag{6}$$

Equation (4) can be depicited in signal-processing terms as shown in Fig. 1. Equation (4a) indicates that $\langle \dot{\phi} \rangle_{t,\tau}$ is found by averaging $\dot{\phi}$ over a time τ. This averaging can be accomplished by passing the signal $\dot{\phi}(t)$ (in the form of a voltage, perhaps) through a filter with a square impulse response, as shown in Fig. 1. The required shape of this response is found by solving (4a), assuming that $\dot{\phi}(t)$ is a unit impulse at $t=0$.[1] Mathematically, this impulse response can be described by

$$h_a(t) = \frac{u(t) - u(t-\tau)}{\tau} = \frac{\mathrm{rect}_\tau\,(t-\tau/2)}{\tau}. \tag{7}$$

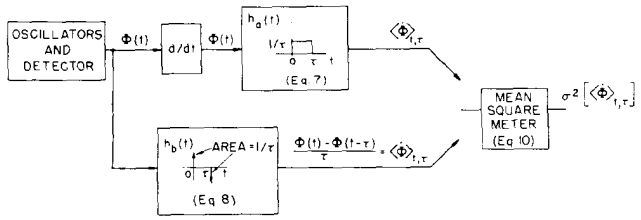

Fig. 1. Representation of (4a) and (4b) in signal-processing terms.

In a similar way, (4b) can be depicted in signal-processing terms as shown in the lower branch of Fig. 1. If we work directly with the phase signal $\phi(t)$, then by inspection the appropriate impulse response in this case contains two impulses, both of area $1/\tau$, as shown. (Again a time delay of $\tau/2$ seconds has been introduced.) This response is described by

$$h_b(t) = \frac{\delta(t) - \delta(t-\tau)}{\tau}. \tag{8}$$

Because both filters h_a and h_b are clearly difficult to realize in practice, systems to measure $\langle \phi \rangle_{t,\tau}$ usually do not conform directly to either of these signal-processing diagrams. Practical systems for measuring $\langle \dot{\phi} \rangle_{t,\tau}$ are presented in Section III.

B. Variance

Because $\phi(t)$, and hence $\phi(t)$ and $\langle \phi \rangle_{t,\tau}$ are random variables, some measure of their dispersion is needed. For this purpose we often calculate the standard deviation σ or the variance σ^2, the latter being defined as

$$\sigma^2[X] = \overline{(X - \bar{X})^2} = \overline{X^2} - (\bar{X})^2 \tag{9}$$

where the bar signifies either time or statistical average. The variance of the frequency averaged over time τ is thus

$$\sigma^2[\langle \phi \rangle_{t,\tau}] = \overline{\langle \phi \rangle_{t,\tau}^2}. \tag{10}$$

Here the variance is identical to the mean-square value because the mean value is zero:

$$\overline{\langle \phi \rangle_{t,\tau}} = \frac{1}{\tau} \int_{t-\tau/2}^{t+\tau/2} \overline{\phi(t')}\, dt' = 0 \tag{11}$$

on the basis that, by definition, $\overline{\phi(t')}$ equals zero. A block corresponding to (10) is included in Fig. 1.

C. Autocorrelation and Spectral Density

The frequency stability of an oscillator can also be specified in terms of autocorrelation functions (also called autocovariance—see, for example, Blackman and Tukey [1]) or spectral densities. Returning for a moment to (1), it is clear that four possible spectra might be of interest in describing the properties of the signal $v(t)$.

1) The complete spectrum of $v(t)$. This is often called the RF spectrum, because it includes the carrier and all sidebands.
2) The spectral density of $A(t)$, which could be found by passing $v(t)$ through an ideal AM detector, and measuring the spectrum of the detector output.
3) $S_\phi(\omega)$, the spectral density of $\phi(t)$, found by passing $v(t)$ through an ideal phase detector, and measuring the detector output spectrum.
4) $S_{\dot{\phi}}(\omega)$, the spectrum of $\phi(t)$, obtained by spectral analysis of the output of an ideal FM detector.

The RF spectrum of $v(t)$ is of great importance in many applications, but for very stable oscillators in which the sidebands are orders of magnitude smaller than the carrier everywhere except close to the carrier, it is often difficult to measure directly. Thus, for stable oscillators the most useful spectral representation of the frequency stability is usually $S_\phi(\omega)$ or $S_{\dot{\phi}}(\omega)$. For the frequently encountered case where the AM power spectral density is negligible, and the mean-square value of the phase is much less than one rad^2, for fre-

[1] For mathematical symmetry, the integrals have been written with limits symmetric about t. However, to insure physical realizability of the filter, the impulse response has been drawn from 0 to τ, implying that the lower and upper limits of integration have been changed to t and $t+\tau$, respectively. This corresponds to a time delay of $\tau/2$ seconds.

quencies greater than some minimum value, the RF power spectral density (two-sided) is

$$S_{RF}(\omega) \approx \frac{P}{2}(S_\phi(\omega + \omega_0) + S_\phi(\omega - \omega_0))$$

where P is the carrier power, and the expression is valid except for the carrier frequencies, $\pm\omega_0$, and narrow bands surrounding them containing all the high modulation-index, low-frequency modulation sidebands. The low modulation-index portion of the power spectral density of the sidebands has the same shape as the phase power spectral density because only the first-order sidebands are of any consequence.

The spectral density of a random signal is defined as the Fourier transform of its autocorrelation function [2]. Thus, we first define the autocorrelation of the phase as

$$R_\phi(\tau) = \overline{\phi(t + \tau/2)\phi(t - \tau/2)} = \lim_{T\to\infty} \frac{1}{T}\int_{-T/2}^{T/2} \phi(t + \tau/2)\phi(t - \tau/2)\, dt \quad (12)$$

where the bar signifies statistical average, and ergodicity is assumed. Similarily, $R_\phi(\tau)$ is the autocorrelation function of the frequency departure

$$R_{\dot\phi}(\tau) = \overline{\dot\phi(t + \tau/2)\dot\phi(t - \tau/2)} = \lim_{T\to\infty} \frac{1}{T}\int_{-T/2}^{T/2} \dot\phi(t + \tau/2)\dot\phi(t - \tau/2)\, dt. \quad (13)$$

Writing these both as functions of τ alone implies that ϕ and $\dot\phi$ are stationary in the wide sense [3].

As pointed out above, the spectral density of the phase (using two-sided spectra) is

$$S_\phi(\omega) = \int_{-\infty}^{\infty} R_\phi(\tau)e^{-j\omega\tau}\, d\tau = 2\int_0^{\infty} R_\phi(\tau)\cos\omega\tau\, d\tau. \quad (14)$$

It also follows that $R_\phi(\tau)$ is the Fourier transform of $S_\phi(\omega)$:

$$R_\phi(\tau) = \frac{1}{2\pi}\int_{-\infty}^{\infty} S_\phi(\omega)e^{j\omega\tau}\, d\omega = \frac{1}{\pi}\int_0^{\infty} S_\phi(\omega)\cos\omega\tau\, d\omega. \quad (15)$$

In a similar way, $S_{\dot\phi}(\omega)$ and $R_{\dot\phi}(\tau)$ also form a Fourier transform pair, identical in form to (14) and (15).

On the basis of our original definitions, $\dot\phi(t)$ was the time derivative of $\phi(t)$. Differentiation in the time domain corresponds to multiplication by $j\omega$ in the frequency domain and, hence, multiplication by ω^2 in terms of spectral densities. Thus

$$S_{\dot\phi}(\omega) = \omega^2 S_\phi(\omega).$$

In dealing with electrical signals it is customary to calculate the *power* spectral density (units of watts/hertz) for signals that exist for all time, and the *energy* spectral density (units of joules/hertz) for signals that exist only for some finite time (pulse signals). Equations (12), (14), and (15) imply that $S_\phi(\omega)$ is a "power" spectral density, even though there is no power involved (the units are actually radians^2 per hertz). In this paper we shall define all spectra in terms of "power" and not "energy." To emphasize this we shall use the somewhat inappropriate term "power spectral density." Also, in what follows we shall always use two-sided spectra.

There are, of course, other spectral representations of frequency stability that are closely related to $S_\phi(\omega)$ and $S_{\dot\phi}(\omega)$. As an example, often the FM noise of a microwave oscillator is specified in terms of the rms voltage measured in a 1-kc bandwidth at the output of a frequency discriminator [27]. Following the convention for frequency-modulated waves, this measurement is plotted as Δf, the rms frequency deviation measured in a 1-kc bandwidth, vs. frequency f_m (the modulating frequency in the sinusoidal case, but the center frequency of the 1-kc measurement passband).

This measurement can be related to $S_{\dot\phi}(\omega)$, the spectral density of the frequency, by noting from (13) that for $\tau = 0$,

$$R_{\dot\phi}(0) = \overline{\dot\phi^2(t)}$$

and, because of the Fourier transform relationship between $R_{\dot\phi}(\tau)$ and $S_{\dot\phi}(\omega)$,

$$R_{\dot\phi}(0) = \frac{1}{2\pi}\int_{\infty}^{\infty} S_{\dot\phi}(\omega)\, d\omega.$$

Combining these two equations, we obtain

$$\overline{\dot\phi^2(t)} \equiv \frac{1}{2\pi}\int_{-\infty}^{\infty} S_{\dot\phi}(\omega)\, d\omega.$$

This result, which in general relates the mean-square value of a function to the total area under its spectral density curve, is a special case of Parseval's Theorem. For the present case, we want the mean-square value of the signal out of a 1-kc filter, and thus the appropriate relation is

$$\overline{\dot\phi^2(t)}\Big|_{1\text{ kc}} \equiv (\Delta f)^2 = \frac{1}{\pi}\int_{2\pi(f_m-500)}^{2\pi(f_m+500)} S_{\dot\phi}(\omega)\, d\omega$$

for a sharp-edged filter. In the case where $S_{\dot\phi}(\omega)$ is fairly constant over the 1-kc bandwidth, we find

$$(\Delta f)^2 \cong 2000 S_{\dot\phi}(\omega).$$

D. Relations Between Variance and Spectral Densities

The two major methods of specifying the frequency stability of an oscillator presented above, namely the variance of the frequency departure averaged over time τ and the power spectral density, are in fact closely related via the autocorrelation function [4], [5] (see Appendix I). Specifically, the variance of the average frequency departure can be written either in terms of $R_\phi(\tau)$ or $R_{\dot\phi}(\tau)$.

$$\sigma^2[\langle\dot{\phi}\rangle_{t,\tau}] = \frac{2}{\tau^2}\left[R_\phi(0) - R_\phi(\tau)\right] \tag{16a}$$

$$= \frac{2}{\tau}\int_0^\tau R_{\dot\phi}(\tau')\left(1 - \frac{\tau'}{\tau}\right)d\tau'. \tag{16b}$$

This variance is often normalized to yield the variance of the average *fractional* frequency departure by dividing both sides of (16) by ω_0^2.

By substituting (15) into (16a), we can eliminate R_ϕ, and, hence, express the variance directly in terms of the power spectral density of frequency or phase. The resulting expressions are

$$\sigma^2[\langle\dot{\phi}\rangle_{t,\tau}] = \frac{1}{2\pi}\int_{-\infty}^{\infty} S_{\dot\phi}(\omega)\frac{\sin^2\omega\tau/2}{(\omega\tau/2)^2}\,d\omega \tag{17a}$$

$$= \frac{2}{\pi\tau^2}\int_{-\infty}^{\infty} S_\phi(\omega)\sin^2\omega\tau/2\,d\omega. \tag{17b}$$

Although $\sigma^2[\langle\dot{\phi}\rangle_{t,\tau}]$ (or its normalized equivalent) is the variance most commonly used in specifying frequency stability, we include for convenience formulas for several other variances written in terms of autocorrelations and spectral densities:

$$\sigma^2[\langle\phi\rangle_{t,\tau}] = \frac{2}{\tau}\int_0^\tau R_\phi(\tau')\left(1 - \frac{\tau'}{\tau}\right)d\tau'$$

$$= \text{variance of average phase} \tag{18}$$

$$\sigma^2[\Delta_\tau\phi] = 2[R_\phi(0) - R_\phi(\tau)]$$

$$= \text{variance of accumulated phase} \tag{19}$$

$$\sigma^2[\phi(t)] = R_\phi(0) = \frac{1}{\pi}\int_0^\infty S_\phi(\omega)\,d\omega$$

$$= \text{variance of phase} \tag{20}$$

$$\sigma^2[\dot\phi(t)] = R_{\dot\phi}(0) = \frac{1}{\pi}\int_0^\infty S_{\dot\phi}(\omega)\,d\omega$$

$$= \text{variance of frequency} \tag{21}$$

$$= \frac{1}{\pi}\int_0^\infty \omega^2 S_\phi(\omega)\,d\omega.$$

The preceding formulas hold for wide-sense stationary random processes or for time functions that have stationary means and autocorrelation functions that depend only on the time difference.

E. Signal-Processing Summary

The interrelations between power spectral density and variance of average frequency departure, which have been stated mathematically above, are shown in signal processing terms in Fig. 2. Thus, the figure serves as a summary of the preceding discussion. Practical methods of performing these data-processing steps are discussed in Section III.

At the top left of Fig. 2 is the system to be analyzed (for example, two crystal oscillators plus phase detector and nulling servo, see Section III-C). We assume that the output from the system is the phase difference, $\phi(t)$. The first row indicates the real-time data processing required to find $\langle\dot\phi\rangle_{t,\tau}$ and its variance, based on Fig. 1. The second row in Fig. 2 shows the data reduction required to specify the oscillator stability in terms of spectral densities, either $S_\phi(\omega)$ or $S_{\dot\phi}(\omega)$. In addition, Fig. 2 shows the steps necessary to find the variance from $S_{\dot\phi}(\omega)$, i.e., (17a). Here, however, we emphasize the relationship between the time-domain operations and the corresponding operations required in the frequency domain. Corresponding to convolution with $h_a(t)$, we have multiplication by $|H_a(j\omega)|^2$, where $H_a(j\omega)$ is the

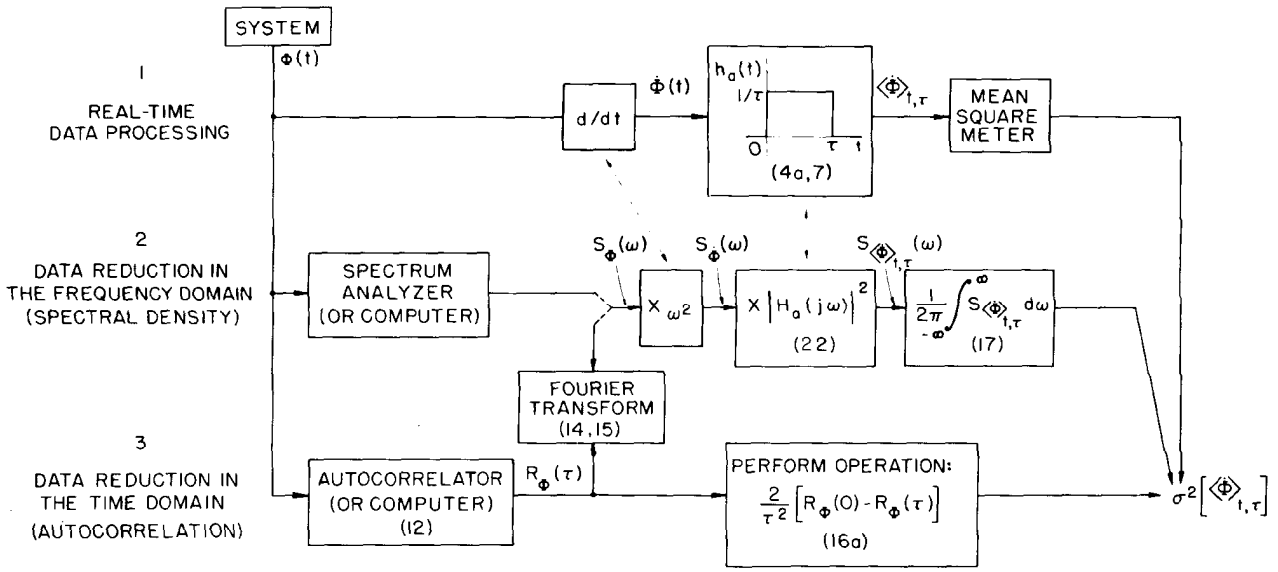

Fig. 2. Summary of methods of data processing. Numbers in brackets refer to equation numbers in the text. Double arrows (<----->) indicate Fourier transform relationship (time <-----> power spectral density).

Fourier transform of $h_a(t)$. Specifically

$$|H_a(j\omega)|^2 = \frac{\sin^2 \omega\tau/2}{(\omega\tau/2)^2}. \tag{22}$$

Thus, we find that the spectral density of $\langle\dot{\phi}\rangle_{t,\tau}$ is

$$S_{\langle\dot{\phi}\rangle_{t,\tau}}(\omega) = S_{\dot{\phi}}(\omega)\,|H_a(j\omega)|^2.$$

Parseval's Theorem states that finding the mean-square value of $\langle\dot{\phi}\rangle_{t,\tau}$ is identical to finding the area under $S_{\langle\dot{\phi}\rangle_{t,\tau}}(\omega)$. The required integration of $S_{\langle\dot{\phi}\rangle_{t,\tau}}(\omega)$ is specified in Fig. 2.

The preceding discussion indicates that the first two rows of Fig. 2 are closely related in that each operation in one row has its counterpart in the other. Thus, the diagram can be traversed not only along the indicated solid lines, but also vertically between corresponding variables in the first two rows. Mathematically this vertical movement is accomplished by applying an appropriate Fourier relation (time ←- - - → spectral density); conceptually we merely move from the time domain to the frequency domain.

The third row in Fig. 2 shows the operations required to find the variance via the autocorrelation function, i.e., (16a).

Figure 2 indicates that there are alternate paths for calculating many of the quantities of interest here. Although for a particular problem one method will usually be much simpler than others, the alternate paths provide a useful check on computations. As an example of such a calculation, assume that $S_\phi(\omega)$ is band-limited white noise, as shown in Fig. 3(a). (This model for a phase power density spectrum is often encountered in frequency standards.) Let us first calculate $\sigma^2[\langle\dot{\phi}\rangle_{t,\tau}]$ following the method outlined in the second row of Fig. 2. First we find $S_{\dot{\phi}}(\omega)$. The result, shown in Fig. 3(b), indicates a predominance of high-frequency noise. The variance can now be found by multiplying $S_{\dot{\phi}}(\omega)$ by $|H_a|^2$ to yield $S_{\langle\dot{\phi}\rangle_{t,\tau}}(\omega)$ and then integrating. Of course, $S_{\langle\dot{\phi}\rangle_{t,\tau}}$ is a function of both ω and the averaging time τ; in this case

$$S_{\langle\dot{\phi}\rangle_{t,\tau}}(\omega) = \begin{cases} \dfrac{4}{\tau^2}\sin^2 \dfrac{\omega\tau}{2} = \dfrac{2}{\tau^2} - \dfrac{2}{\tau^2}\cos\omega\tau, & -\omega_c < \omega < \omega_c \\ = 0 & \text{elsewhere} \end{cases}.$$

From Fig. 2

$$\sigma^2[\langle\phi\rangle_{t,\tau}] = \frac{1}{2\pi}\int_{-\omega_c}^{\omega_c}\left(\frac{2}{\tau^2} - \frac{2}{\tau^2}\cos\omega\tau\right)d\omega.$$

Without performing the integration, we can see that for large τ, the first integral will dominate, and thus

$$\sigma^2[\langle\phi\rangle_{t,\tau}] = \frac{2\omega_c}{\pi\tau^2} \qquad (\omega_c\tau \gg 2\pi).$$

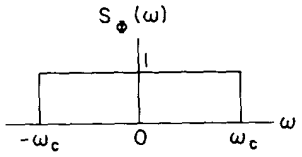

(a)

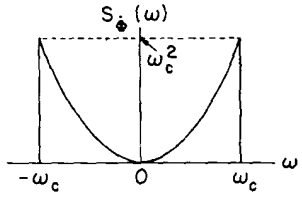

(b)

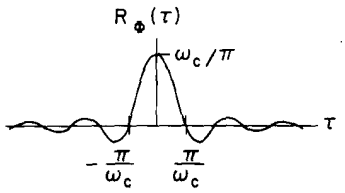

(c)

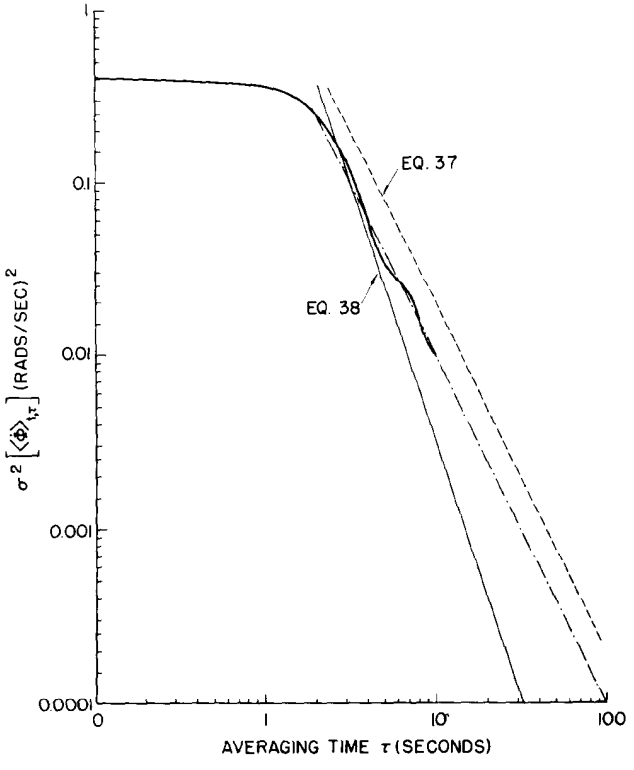

(d)

Fig. 3. Example: calculation of $\sigma^2[\langle\dot{\phi}\rangle_{t,\tau}]$ for band-limited white phase noise. (a) Power density spectrum of phase, rad²/hertz. (b) Power density spectrum of frequency, (rad/s)²/hertz. (c) Autocorrelation of phase, rad². (d) Variance of average frequency, (rad/s)².

Also, for τ very small, the $H_a(j\omega)$ function is approximately flat over the range $-\omega_c<\omega<\omega_c$, so multiplication by $|H_a|^2$ leaves S_ϕ relatively unchanged. Thus, in this case

$$\sigma^2 = \frac{1}{2\pi}\int_{-\omega_c}^{\omega_c} \omega^2\, d\omega = \frac{\omega_c^3}{3\pi} \qquad (\omega_c\tau \ll 1).$$

The third row of Fig. 2 indicates that an alternative method of finding the variance is via the autocorrelation. Because $S_\phi(\omega)$ is a square pulse of unit height and length $2\omega_c$, we find from (15) that

$$R_\phi(\tau) = \frac{\omega_c}{\pi}\left[\frac{\sin \omega_c\tau}{\omega_c\tau}\right]$$

as shown in Fig. 3(c). Equation (16a) indicates that the variance can be found by multiplying the difference between $R_\phi(\tau)$ and its value at $\tau=0$ by the factor $2/\tau^2$. The result is shown in Fig. 3(d); here ω_c, the width of the noise spectrum, has been arbitrarily set equal to $\pi/2$ for ease of calculation. Note that the general shape of the variance can be sketched by inspection as a basic $1/\tau^2$ behavior perturbed by the autocorrelation difference term. As a check on previous calculations, we see that because $R_\phi(\tau)$ approaches zero for large τ,

$$\sigma^2[\langle\phi\rangle_{t,\tau}] = \frac{2}{\tau^2}\,[R_\phi(0)] = \frac{2\omega_c}{\pi\tau^2} \qquad (\omega_c\tau \gg 2\pi)$$

as before.

F. Finite Data Length

The preceding derivations and discussion have all been based on the assumption that the functions $\phi(t)$ and $\dot\phi(t)$ exist for all time. In practice this is not so; measurements can only be made over some finite time T. Under these conditions we can only make *estimates* of σ and S. These estimates (denoted $\hat\sigma$, $\hat S$) are themselves statistical variables, with variances and all other properties associated with random processes. This problem is treated in Appendix II, and at greater length in Allan [6]. From Appendix II, (76), the average value of the variance of average frequency departure is

$$\overline{\hat\sigma^2[\langle\phi\rangle_{t,\tau}]} = \frac{1}{2\pi}\int_{-\infty}^{\infty} S_{\langle\dot\phi\rangle_{t,\tau}}(\omega)\left(1-\frac{\sin^2\omega(T-\tau)/2}{[\omega(T-\tau)/2]^2}\right)d\omega. \qquad (23)$$

The corresponding relation for the case of continuous data is, from Fig. 2,

$$\sigma^2[\langle\dot\phi\rangle_{t,\tau}] = \frac{1}{2\pi}\int_{-\infty}^{\infty} S_{\langle\dot\phi\rangle_{t,\tau}}(\omega)\, d\omega.$$

Equation (23) differs from this expression, in that effectively the low-frequency portion of the spectrum of $S_{\langle\dot\phi\rangle_{t,\tau}}$ (i.e., below $\omega\cong 2/T$) is removed before the integration.

Clearly, the effect of the variance of measuring $\phi(t)$ for only a finite time T will depend on the shape of the spectral density. Specifically, if $S_{\langle\dot\phi\rangle_{t,\tau}}$ is relatively wideband, such that most of the power is at frequencies higher than $\omega\cong 2/T$, then the variance is not going to be appreciably affected by the finite measurement time T. On the other hand, if $S_{\langle\dot\phi\rangle_{t,\tau}}$ is relatively narrow-band, or is greatly peaked at low frequencies, then the apparent variance based on data over time T is going to be considerably smaller than the true variance. As an example of this, in the case of $1/f$-frequency noise (i.e., $S_{\dot\phi}(\omega) = k/\omega$), the true variance is finite, whereas a finite observation time always gives a finite result for $\overline{\hat\sigma^2}$ (see Appendix II).

We can assess from a signal-processing point of view the effect on the spectral densities S_ϕ and $S_{\dot\phi}$ of making measurements for a finite rather than infinite time. In the time domain, phase data acquisition for a length of time T can be represented by multiplying the signal $\phi(t)$ (assumed to exist for all time), by a pulse of unit height extending from $-T/2$ to $T/2$. The corresponding operation in the frequency domain is convolution with the function

$$|H_c(j\omega)|^2 = \frac{T\sin^2\omega T/2}{(\omega T/2)^2} = Q_c(\omega) \qquad (24)$$

(see Appendix II).

For example, the average value of the estimate of the phase spectral density is

$$\overline{\hat S_\phi(\omega)} = S_\phi(\omega) \otimes |H_c(j\omega)|^2 \qquad (25)$$

where the symbol $\otimes$ indicates convolution. Thus, the effect of finite data length is to blur the spectrum somewhat, thereby making it impossible to resolve frequency components on a finer scale than $\Delta\omega\cong 2/T$ (see Appendix II).

III. Measurement Techniques

There are several well-known techniques for making measurements of some of the quantities described above. Some of these will now be considered.

A. Multiple-Period Technique

The general system of a multiple-period measurement is shown in Fig. 4. Two signal sources slightly offset in average frequency feed two identical channels through optional frequency multipliers to a mixer. (The multipliers may be used to increase the resolution and sensitivity of the measurement.) The counter then measures the period of the mixer output.

The output from the mixer contains all the desired frequency and phase information. That is, if the two signal sources have exactly the same statistics for $\phi_1(t)$ and $\phi_2(t)$ but are uncorrelated, then all the fluctuation may be assumed to be in one channel $\sqrt{2}$ times as large as that channel alone, while the other channel may be assumed to be perfect.

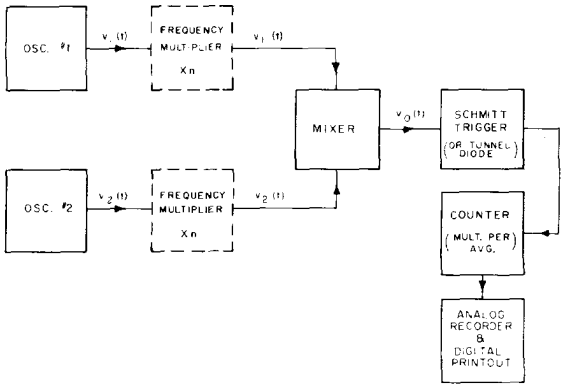

Fig. 4. Multiple-period measuring system.

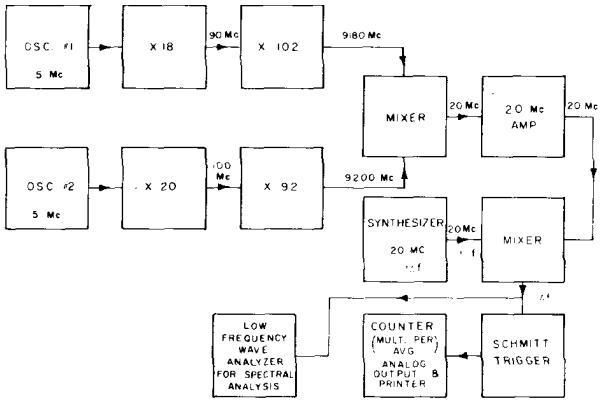

Fig. 5. Versatile multiple-period measuring system.

Thus, we can assume the mixer output signal to be of the form

$$v_0(t) = A \cos (\omega_0 t + \phi(t)) \tag{26}$$

where A, ω_0 and ϕ are as defined in (1), except that here ω_0 represents the constant frequency *difference* between the two oscillators, and ϕ is the phase *difference*. The period of the mixer output waveform is measured by using a counter to determine the time τ required for N_0 periods of $v_0(t)$. The relation between the counter output τ and the phase is

$$2\pi N_0 = \omega_0 \tau + \phi(\tau) - \phi(0). \tag{27}$$

Note that, in this method, the time τ is not constant. In fact, τ is the quantity that carries the information about the phase variations. Specifically, let

$$\tau_0 = \frac{2\pi N_0}{\omega_0} \tag{28}$$

and

$$\tau = \tau_0 - \Delta\tau. \tag{29}$$

Then (27) reduces to

$$\phi(\tau) - \phi(0) = \omega_0 \Delta\tau. \tag{30}$$

If $\omega_0 \Delta\tau \ll 1$ and $\dot{\phi}(0)\Delta\tau \ll 1$, then only very small error is caused by replacing $\phi(\tau)$ by $\phi(\tau_0)$. (The process of averaging over many measurements helps here.) The multiple-period technique thus measures essentially $\phi(t+\tau_0) - \phi(t)$. Dividing by τ_0 to reduce it to the form of (4), we thus obtain from (30)

$$\frac{\phi(t + \tau_0) - \phi(t)}{\tau_0} = \langle \phi \rangle_{t,\tau 0} \cong \frac{\omega_0 \Delta\tau}{\tau_0}. \tag{31}$$

Thus the mixer-counter combination does, in fact, perform the function described by (4) and Fig. 1. The standard deviation of $\langle \dot{\phi} \rangle_{t,\tau_0}$ can be found by making repeated measurements:

$$\sigma[\langle \phi \rangle_{t,\tau_0}] = \frac{\omega_0 \sigma[\Delta\tau]}{\tau_0}. \tag{32}$$

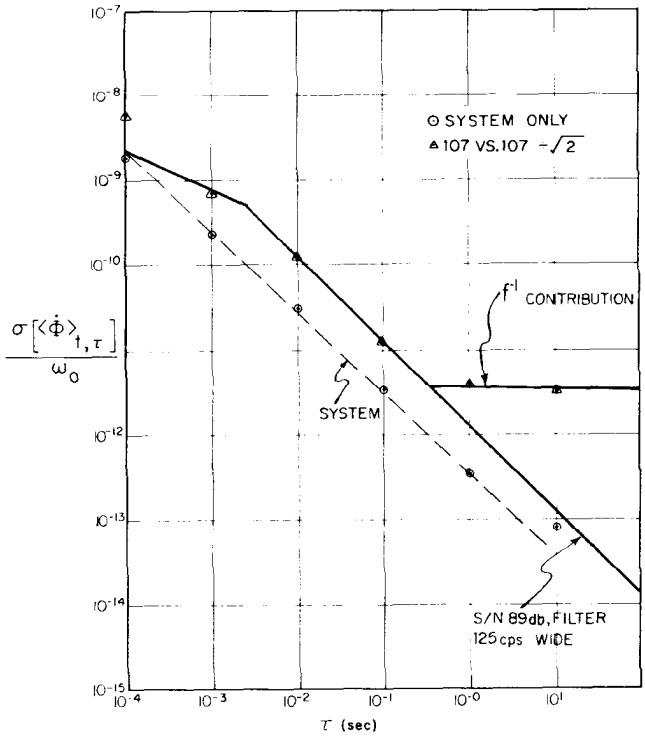

Fig. 6. Measurements with multiple-period system.

Figure 5 shows a block diagram of a versatile system that allows the two oscillators to have zero offset. This feature permits the system noise to be evaluated by feeding both channels from one source. The offset is obtained by the frequency synthesizer whose fluctuations do not greatly degrade the measurement, since the oscillator fluctuations have been multiplied by 1840 in the 20 Mc/s difference frequency before the comparison is made. Figure 6 shows some typical results obtained with this system.

From a practical standpoint the system gives good results for averaging times greater than 10^{-4} seconds, and is particularly good for times greater than 10^{-2} seconds.

B. Phase Detector Techniques [7], [8]

Figure 7 shows a typical phase detector or multiplier measurement technique. If the two signals are identical in frequency and are placed in quadrature they may be represented as

$$v_1(t) = A_1(t) \cos(\omega_0 t + \phi_1(t)),$$
$$v_2(t) = A_2(t) \sin(\omega_0 t + \phi_2(t)). \tag{33}$$

If the difference between $\phi_2(t)$ and $\phi_1(t)$ is small, the phase detector output will be

$$v_0(t) \cong \frac{A_1(t)A_2(t)}{2}\phi(t) \tag{34}$$

if we designate the phase difference $\phi_2(t)-\phi_1(t)$ as $\phi(t)$. If the variations in A_1 and A_2 are small, as is usually the case, they may be neglected and the phase detector output is essentially the difference between the instantaneous phases. Both signals may be heterodyned down to a convenient low frequency by means of two mixers and a common local oscillator. Because this phase detector is linear only for small angles, measurements can be taken only for time intervals during which the phase difference $\phi(t)$ is less than $\pi/6$. Within this restriction, the phase detector output may be analyzed by a low-frequency narrow-band wave analyzer to estimate the spectral density of the phase $S_\phi(\omega)$ directly. Alternatively, an rms voltmeter can be used to estimate $\sigma[\phi(t)]$.

Often it is desirable to place some form of network at the phase detector output in order to have the voltmeter read $\sigma[\langle\dot{\phi}\rangle_{t,\tau}]$ directly. To find $\sigma[\langle\dot{\phi}\rangle_{t,\tau}]$ exactly, Fig. 2 indicates that the required network is a differentiator followed by a filter with a response

$$|H_a(j\omega)|^2 = \frac{\sin^2 \omega\tau/2}{(\omega\tau/2)^2}.$$

Clearly, the $(\sin x)/x$ response is difficult to approximate with a simple RLC filter; thus it is appropriate to discuss two other filters that might be used as substitutes. The first is a simple single-pole low-pass filter, with a frequency response $H_d(j\omega)$ equal to

$$H_d(j\omega) = \frac{1}{1 + j\omega\tau/2}. \tag{35}$$

The second is a multiple-pole, sharp-cutoff filter with response approaching

$$\left.\begin{aligned} H_e(j\omega) &= 1, \quad -\omega_0 < \omega < \omega_0 \\ &= 0 \quad \text{elsewhere} \end{aligned}\right]. \tag{36}$$

Using H_d, the corresponding equations for the variances are as follows.

$$\sigma_d^2 = \frac{1}{2\pi}\int_{-\infty}^{\infty} S_{\dot{\phi}}(\omega)\,\frac{1}{1 + (\omega\tau/2)^2}\,d\omega \tag{37}$$

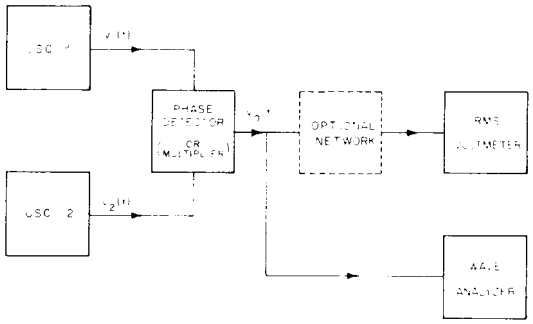

Fig. 7. Phase detector system.

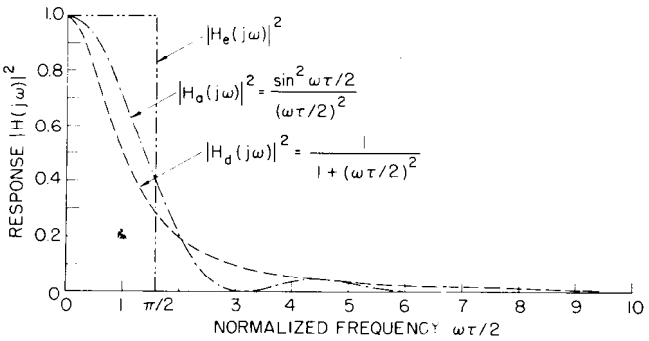

Fig. 8. Frequency response of three filters.

and using H_e

$$\sigma_e^2 = \frac{1}{2\pi}\int_{-\omega_0}^{\omega_0} S_{\dot{\phi}}(\omega)\,d\omega. \tag{38}$$

Because the filter characteristic of interest is $|H(j\omega)|^2$, the squared magnitude of response for each of the three filters in question is plotted in Fig. 8. Because σ^2 is proportional to the area under the power spectral density curve, the three characteristics in Fig. 8 have been normalized to have the same area. This requires that the square filter, (36), have a bandwidth $\omega_0 = \pi/\tau$.

Figure 8 can now be used as a basis for comparing σ_d^2 and σ_e^2 with the true variance $\sigma^2[\langle\dot{\phi}\rangle_{t,\tau}]$. First, all three functions have the same area, so σ_d^2 and σ_e^2 will be identical to the true variance if $S_{\dot{\phi}}(\omega)$ is flat for all frequencies. Second, all three functions have about the same ordinates for small $\omega\tau/2$. Thus, the variances measured for values of τ that make the filters much broader than the spectrum of $S_{\dot{\phi}}(\omega)$ will be about the same for the three filters. Specifically, if $S_{\dot{\phi}}(\omega)$ is band-limited to frequencies below ω_c, then the values of σ_d^2 and σ_e^2 measured for $\tau \ll 2/\omega_c$ will again agree closely with the true value.

Figure 8 indicates that significant divergence in results can be expected when $\omega\tau/2$ is large. In this range, $|H_d|^2$ still has the correct general behavior, i.e., it varies as $1/\omega^2$, but the area is about a factor of two larger than is required. On the other hand, the H_e filter bears no relation to the required $(\sin^2 x)/x^2$ behavior. Thus if

$S_\phi(\omega)$ is peaked at high frequencies, we can expect σ_d^2 measured for large τ to be about a factor of two larger than the true value. Under the same conditions, however, σ_e^2 measured for large τ can be less than the true value by orders of magnitude, depending on the specific constants involved.

To illustrate some of these points, the example in Section II-E involving a flat band-limited phase spectrum has been reworked using the H_d and H_e filters as approximations to the desired H_a filter. The asymptotic results for σ^2 are as follows:

Filter	σ^2	
	$\tau \ll 2/\omega_c$	$\tau \gg 2\pi/\omega_c$
$H_a(j\omega)$ (true dependence)	$\frac{\omega_c^3}{3\pi}$	$\frac{2\omega_c}{\pi\tau^2}$
$H_d(j\omega)$	$\frac{\omega_c^3}{3\pi}$	$\frac{4\omega_c}{\pi\tau^2}$
$H_e(j\omega)$	$\frac{\omega_c^3}{3\pi}$	$\frac{\pi^2}{3\tau^3}$

These results are consistent with the preceding general discussion.

The large τ asymptotes for these cases have been added to Fig. 3(d) to facilitate the intercomparison among the filters. Note particularly in this example that for large τ, σ_d^2 is a factor of 2 large, whereas the calculation based on H_e yields a σ_e^2 which varies as τ^{-3} instead of τ^{-2}. Thus σ_e^2 is too small, i.e., *optimistic*, by a factor that increases linearly with averaging time τ.

We conclude, therefore, that for calculating $\sigma^2[\langle\dot{\phi}\rangle_{t,\tau}]$ the simple one-pole low-pass filter, (35) is a reasonable approximation to the required $(\sin x)/x$ filter, but serious errors may be introduced if a sharp-cutoff filter, (36), is used as the approximation. It is certainly perfectly valid to place a sharp filter at the output of the phase detector and measure the rms voltage appearing at the filter output as an indirect measurement of $S_{\dot{\phi}}(\omega)$ (see, for example, [7]). The error appears when one tries to identify this rms voltage with $\sigma[\langle\dot{\phi}\rangle_{t,\tau}]$.

C. Elapsed Phase Difference Method

Figure 9 shows a block diagram of a simple elapsed phase difference measurement system. The two signals are heterodyned down by means of a common local oscillator to a convenient low frequency suitable for the resolver phase shifter. The servo system maintains the output phase from the phase shifter in fixed relation to the phase in the other channel. Consequently, the phase shift introduced by the phase shifter is equal to the relative phase difference in the two channels.

Since the relative phase is preserved in the heterodyning process, it is equal to the relative phase of the two oscillators. The phase shift may be read electrically by

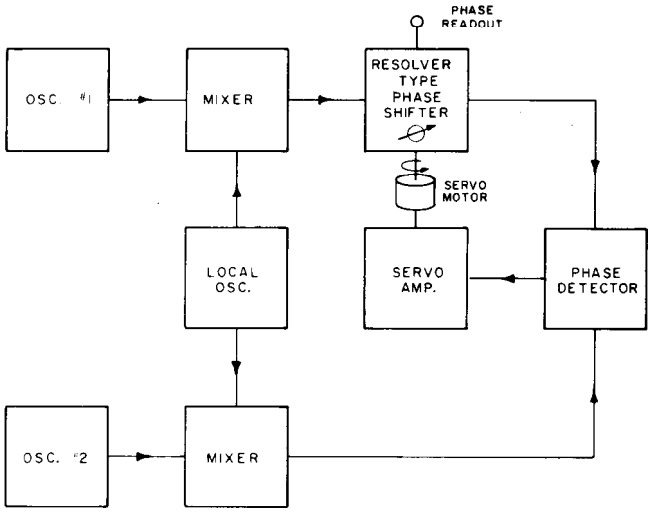

Fig. 9. Elapsed phase method.

an optical shaft encoder and thus fed directly to computation devices. If the phase is read at intervals of time τ, this technique gives an estimate of $\Delta_\tau\phi(t)$ and hence can be used as a basis of computation of $\langle\dot{\phi}\rangle_{t,\tau}$. If the oscillators being compared operate at 5 Mc/s and the resolver encoder can be read to 0.005 of one revolution, the sensitivity is 10^{-12} in $\langle\dot{\phi}\rangle_{t,\tau}/\omega_0$, for a τ of 1000 seconds.

Because of the slow speed of the servo, the high-frequency components of the spectrum do not appear at the encoder output. Some of the high-frequency components can be recovered by measuring the servo-error signal out of the phase detector, provided that a suitable filter is added to compensate for the response of the servo motor.

As pointed out above, the resolver system is readily adaptable to digital computation of oscillator stability. One such method is to calculate $R_\phi(\tau)$ from $\phi(t)$ as provided at the encoder output, and hence calculate $S_\phi(\omega)$ and $\sigma[\langle\dot{\phi}\rangle_{t,\tau}]$. Typical results are shown in Fig. 10 [9]. The phase difference between two 262-MHz signals was sampled and recorded digitally on punched tape every 10 seconds for about ten hours. A plot of the sampled phase is shown in Fig. 10(a). The computer-generated plot of the autocorrelation of the phase is shown in Fig. 10(b). Although the calculation was made for delay times as large as 10 000 seconds, the plot has significant error (because of the finite data length T) beyond $T/10 = 3500$ seconds.

To conserve computer time, the power spectral density of phase, Fig. 10(c), was calculated by forming the Fourier transform of a 1000 point sample of Fig. 10(a). A Hamming routine was used to smooth the resulting spectrum. (See Blackman and Tukey [1].) In spite of the finite data length, we assume that the spectrum thus obtained is approximately the true power spectral density within the limitations discussed in Section II-F.

The curve of standard deviation vs. averaging time, Fig. 10(d), was formed from Fig. 10(b) using (16a).

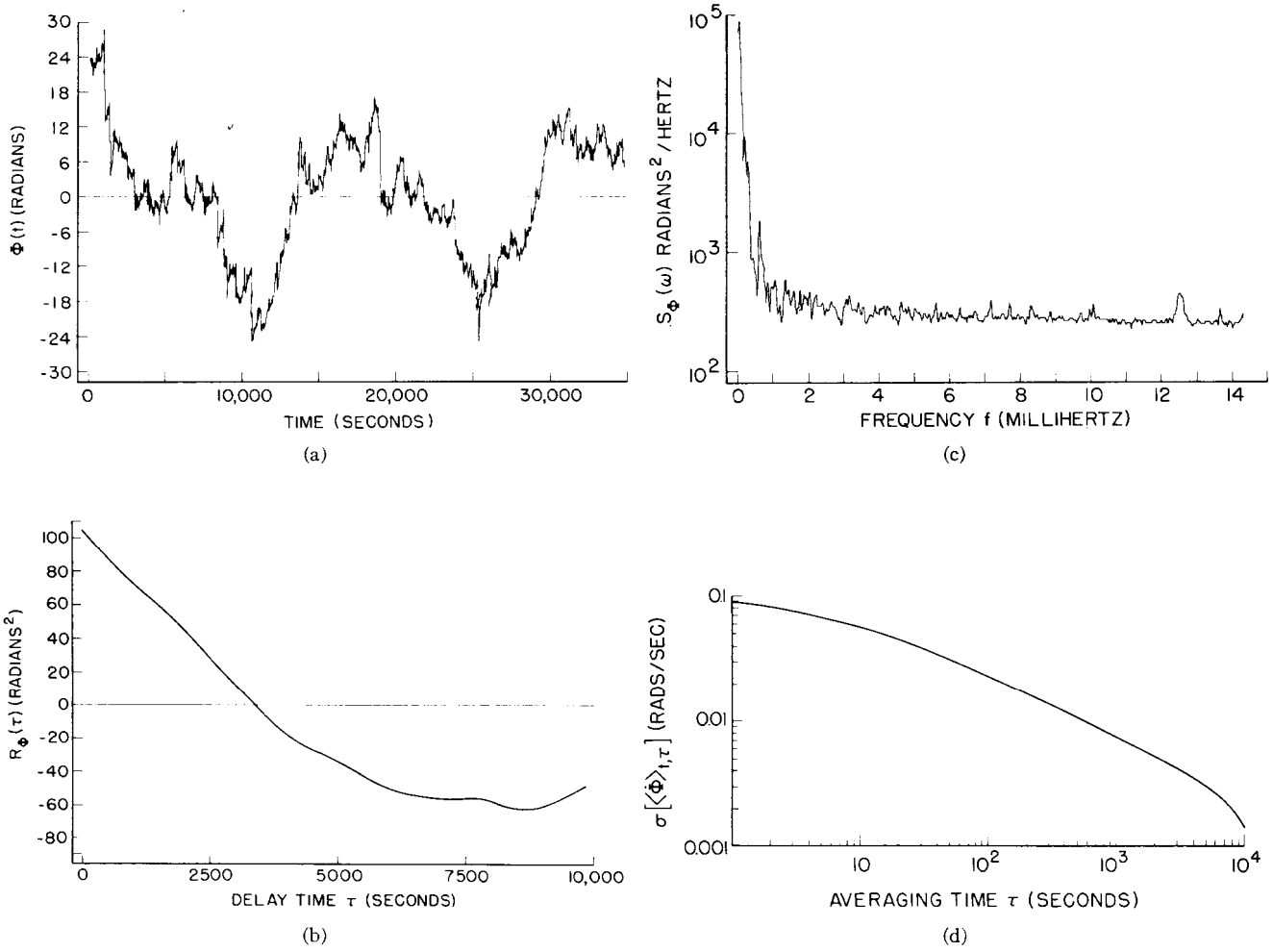

Fig. 10. Computer analysis of 10 hour length of phase data. (a) Phase difference measured at 262 MHz. (b) Autocorrelation of phase difference. (c) Power spectral density of phase. (d) Standard deviation of average frequency.

IV. Noise in Oscillators

Practical oscillators appear to have three main sources of noise contributing to frequency fluctuations. These are: A. additive noise associated with the oscillator and accessory circuits, such as AGC and amplifiers, which does not perturb the oscillation but is merely added to the signal; B. thermal and shot noise in the oscillator itself which actually perturbs the oscillation; and C. fluctuations in the resonator frequency either in the resonator itself or due to circuit parameter changes influencing the resonance frequency. The frequency fluctuations of an oscillator due to the last mentioned source appear to have an f^{-1} power spectral density [10].

A. Additive Noise

In oscillators used for quartz frequency standards, great care is taken to couple very lightly into the oscillating circuit, and because of the nonlinearity of the resonator [11] it is necessary to stabilize the oscillation at a very low power level (typically about 10^{-7}–10^{-6} watts). The nonlinearity causes a coefficient of about 1×10^{-9} per dB of drive at 50 μA in a 2.5-Mc/s fifth overtone crystal [12]. As a consequence, the noise of the amplifiers following the oscillator is the predominant factor for fluctuations involving times of the order of 0.1 second or less.

Assume that the additive noise is band limited by a narrow-band filter with transfer function

$$H(\omega) \simeq \frac{1}{1 + j\dfrac{\omega - \omega_0}{\omega_1}} \tag{39}$$

where ω_1 is the half bandwidth of the filter. As will be shown, this is often a desirable procedure. Such a transfer function, of course, is not realizable but is a good approximation for the narrow-band case. Assume also that the additive noise is white and has a power spectral density S_0. Then the power spectral density of the noise out of the filter will be

$$\frac{S_0}{1 + \left(\dfrac{\omega - \omega_0}{\omega_1}\right)^2}.$$

The total noise power will be

$$P_N = \frac{1}{2\pi}\int_{-\infty}^{\infty} \frac{S_0}{1 + \left(\frac{\omega - \omega_0}{\omega_1}\right)^2} d\omega = \frac{\omega_1 S_0}{2} . \quad (40)$$

If the total signal power P_S is large in comparison to P_N so $P_N/P_S \ll 1$ then it is well known that half the noise power appears as amplitude modulation sidebands on the signal centered in the noise and the other half as phase modulation sidebands. The power spectral density of this effective phase modulation is then

$$S_\phi(\omega) = \frac{1}{\omega_1}\frac{P_N}{P_S}\frac{{\omega_1}^2}{\omega^2 + {\omega_1}^2} \quad (41)$$

and the autocorrelation function is

$$R_\phi(\tau) = \frac{P_N}{P_S}\frac{e^{-\omega_1|\tau|}}{2} . \quad (42)$$

From this, using (16a),

$$\frac{\sigma(\langle\dot{\phi}\rangle_{t,\tau})}{\omega_0} = \frac{1}{\omega_0\tau}\left[\frac{P_N}{P_S}(1 - e^{-\omega_1\tau})\right]^{1/2} \quad (43)$$

(for a single filter). A normalized plot of the asymptotes of this function is shown in Fig. 11. For $\omega_1\tau \gg 1$,

$$\frac{\sigma}{\omega_0} \simeq \frac{1}{\omega_0\tau}\left(\frac{P_N}{P_S}\right)^{1/2};$$

for $\omega_1\tau \ll 1$,

$$\frac{\sigma}{\omega_0} \simeq \frac{1}{\omega_0}\left(\frac{\omega_1}{\tau}\frac{P_N}{P_S}\right)^{1/2} .$$

For $\omega_1\tau \gg 1$, σ/ω_0 is proportional to ${\omega_1}^{1/2}$ for constant noise spectral density and for $\omega_1\tau \ll 1$ it is proportional to ω_1. Consequently, using a narrow-band filter can greatly improve short-term stability. For two cascaded filters each of half-bandwidth ω_1 the result is

$$\frac{\sigma(\langle\dot{\phi}\rangle_{t,\tau})}{\omega_0} = \frac{1}{\omega_0\tau}\left\{\frac{P_N}{P_S}(1 - e^{-\omega_1\tau}(\omega_1\tau + 1))\right\}^{1/2} \quad (44)$$

(for a double filter).

In this case σ is constant for $\omega_1\tau \ll 1$. For any shape of band-pass filter with white additive noise

$$\frac{\sigma}{\omega_0} \simeq \frac{1}{\omega_0\tau}\left(\frac{P_N}{P_S}\right)^{1/2}$$

when τ is much greater than the reciprocal half bandwidth.

As a practical example, consider a 5-Mc/s oscillator followed by a single filter of half bandwidth of 62.5 c/s and $P_N/P_S = -87$ dB. Then for $\tau = 1$ second, $\sigma(\langle\dot{\phi}\rangle_{t,\tau})/\omega_0 = 1.4 \times 10^{-12}$. For a comparison with experimental results see Figs. 6 and 12.

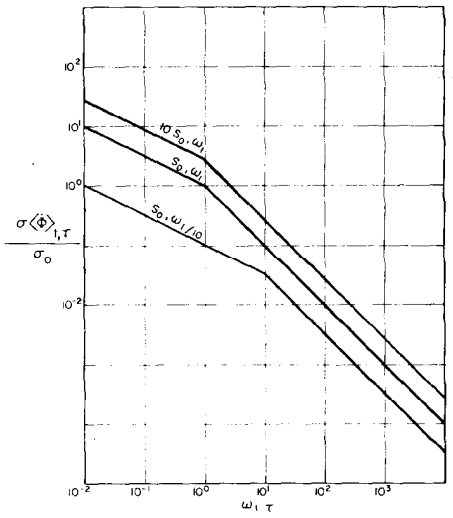

Fig. 11. Normalized additive noise contributions.

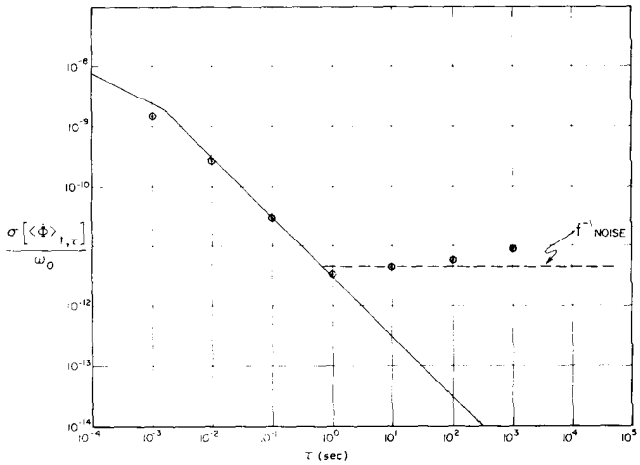

Fig. 12. Theoretical and experimental standard deviation of average fractional frequency departure for a 5.0-Mc/s precision quartz oscillator.

B. *Noise that Perturbs the Oscillation*

The perturbing effects of thermal and shot noise in oscillators are well known [13]. The phase does a random walk due to the perturbations. It has been shown that this leads to

$$\frac{\sigma(\langle\dot{\phi}\rangle_{t,\tau})}{\omega_0} = \left(\frac{kT}{2PQ^2\tau}\right)^{1/2} \quad (45)$$

where

k = Boltzmann's constant
T = the effective noise temperature
P = the total power delivered to the resonator and the load, and
Q = the loaded Q of the resonator.

As an example consider a 5-Mc/s oscillator with $Q = 2 \times 10^6$, $P = 10^{-7}$ watts, and $T = 10^{3°}$ K. For $\tau = 1$ second $\sigma(\langle\dot{\phi}\rangle_{t,\tau})/\omega_0 = 1.3 \times 10^{-13}$. From this example and

the previous one, it is apparent that the additive noise will dominate over perturbation noise for short averaging times in precision crystal oscillators. Here the effects of the two sources of noise would become equal at an averaging time of about 100 seconds with a total fluctuation of about 2×10^{14} if no other sources were effective. For times longer than 100 seconds, the perturbation type noise would dominate.

C. f^{-1} Noise

The third main source of noise is that which has an f^{-1} power spectral density of frequency fluctuation, i.e., $S_\phi(\omega)=K/|\omega|$, K a constant. In addition to this, oscillators drift in frequency (drift is usually accompanied by an f^{-1} power spectral density). Because of the drift in frequency, the phase is not a stationary process. Also, since an f^{-1} power spectral density for frequency fluctuations corresponds to $S_\phi(\omega)$ proportional to $|\omega|^{-3}$,

$$\sigma^2(\langle\dot{\phi}\rangle_{t,\tau})=\frac{1}{\pi\tau^2}\int_{-\infty}^{\infty}S_\phi(\omega)(1-\cos\omega\tau)\,d\omega$$

[from (16a) with the autocorrelation functions written in terms of $S_\phi(\omega)$ using (15)] does not converge since $1-\cos\omega\tau$ only goes to zero as ω^2 for ω approaching zero. This is not surprising. If the f^{-1} spectrum persisted down to zero frequency we would see infinitely large fluctuations by observing over all time.

In the actual situation observations are made over a finite time T. If the frequency drift is removed during the time T by subtraction of the least squares fit of a straight line, this behaves like a high-pass filter acting on the low-frequency components of the phase (see Appendix II). The output of this filter goes to zero as ω^2 for ω approaching zero, and the filter starts to cut off at $\omega\simeq2/T$. This gives finite results for $\sigma(\langle\dot{\phi}\rangle_{t,\tau})/\omega_0$ as shown in Appendix II. It is apparent from the functional form of the integral that if the ratio of observing time to averaging time T/τ is constant (corresponding to a fixed number of samples) then $\sigma(\langle\dot{\phi}\rangle_{t,\tau})/\omega_0$ is constant. Since there is no theory giving the strength of the f^{-1}-spectral density, no prediction can be made as to the constant value of σ. The dependence of σ^2 on T/τ is proportional to $1.04+\frac{1}{2}\log T/2\tau$.

Actual oscillators measured under the conditions of finite T and removal of drift exhibit the predicted behavior (see Figs. 6 and 12). For T/τ of about 100, $\sigma(\langle\dot{\phi}\rangle_{t,\tau})/\omega_0$ flattens out at a value somewhat greater than 1×10^{-12}. Since this is larger than the fluctuations due to the perturbing type of noise at the τ for which additive noise becomes dominant, it is apparent that the effects of the perturbing type of noise are not seen at all in many frequency standards. Figure 13 shows the effects due to the three sources of fluctuations.

J. Barnes [14] of the NBS Laboratories, Boulder, Colo., has recently shown that taking successive differences of the phase has interesting consequences. For example, taking second differences removes the linear frequency drift and also gives convergent results inde-

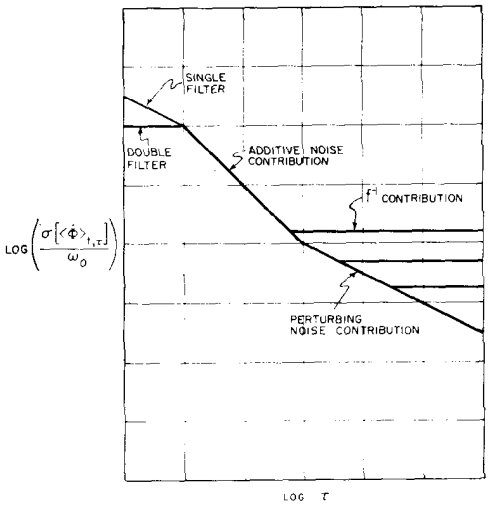

Fig. 13. Contributions to oscillator fluctuations.

pendent of observation time for an assumed f^{-1}-pow spectrum. As shown in Appendix I

$$\sigma\left(\frac{\Delta_\tau^2\phi(t)}{\omega_0\tau}\right)=\frac{1}{\omega_0\tau}\left[6R_\phi(0)-8R_\phi(\tau)+2R_\phi(2\tau)\right]^{1/2} \quad (4$$

where $\Delta_\tau^2\phi(t)\equiv\phi(t+\tau)-2\phi(t)+\phi(t-\tau)$ is the seco phase difference. Using this on an f^{-1}-power spectr density of frequency fluctuations, $S_\phi(\omega)=K/|\omega|^3$, giv

$$\sigma=\frac{(8K\log 2)^{1/2}}{\omega_0}. \quad (4$$

Since this is independent of observation time T, it a pears to be a good measure for the f^{-1} characteristic oscillators.

D. Noise in Masers

It is interesting to compute the effects of the perturl ing thermal noise and additive noise in maser oscillator Following Kleppner et al. [15], [16], but solving tl first-order perturbation exactly and correcting th thermal noise expression [17] gives a total spectral der sity of phase (two-sided) for a hydrogen maser.

$$S_\phi(\omega)=\frac{kT}{2P}\left(\frac{Q_e}{Q_{e,l}}+\frac{\omega_0^2}{\omega^2Q_l^2}G_e(\omega)\right). \quad (4$$

Here

k = Boltzmann's constant
T = absolute temperature
P = power delivered by the beam to the loade cavity
Q_e = external cavity Q
$Q_{e,l}$ = loaded cavity Q
Q_l = atomic line $Q=\omega_0/2\gamma$, and
$G_e(\omega)=\omega_1^2/(\omega^2+\omega_1^2)$, the equivalent low-pass mag nitude squared impedance function of th cavity, where $\omega_1=\omega_0/(2Q_{e,l})$.

In deriving (48) it is assumed that the maser is coupled to its load through an isolator in thermal equilibrium with the cavity and consequently the available signal power is $P_0 = P(Q_{c,l}/Q_c)$ and the available noise power spectral density is just $(kT)/2$. The first term in (48) is just the additive noise (white phase noise) and the second term (low-pass filtered white frequency noise) arises from the perturbation of the oscillation. Note that for $\omega > (\omega_0/Q_l)(Q_{c,l}/Q_c)^{1/2}$, the additive noise predominates. It is interesting to note that a portion of the additive noise term is actually present in the solution to the maser signal in the cavity [17]. This is similar to results obtained by Hafner [18] for an oscillator with two coupled tuned circuits.

The corresponding result for the rubidium maser has not yet been derived, but the mechanism of operation is very similar so that the result is probably the same except that P should be replaced by the power delivered to the loaded cavity by the rubidium atoms. We will assume here that the results are valid for the rubidium maser.

Since the additive white phase noise term in (48) is very broadband, most applications involving the maser will require that the bandwidth of the output be restricted. If the system has an effective single tuned bandpass characteristic of width $2\omega_1'$ with $\omega_1' \ll \omega_1$, and a noise factor F (referred to the maser input port), we obtain

$$\frac{\sigma(\langle\dot{\phi}\rangle_{t,\tau})}{\omega_0} = \left\{\frac{kT}{2P}\left[\frac{F\omega_1' Q_e}{\omega_0^2\tau^2 Q_{c,l}}(1 - e^{-\omega_1'\tau}) + \frac{1}{Q_l^2\tau}\left(1 - \frac{(1 - e^{-\omega_1'\tau})}{\omega_1'\tau}\right)\right]\right\}^{1/2}. \quad (49)$$

For $\omega_1'\tau \gg 1$ this reduces to

$$\frac{\sigma(\langle\dot{\phi}\rangle_{t,\tau})}{\omega_0} \approx \left\{\frac{kT}{2P}\left[\frac{F\omega_1' Q_e}{\omega_0^2\tau^2 Q_{c,l}} + \frac{1}{Q_l^2\tau}\right]\right\}^{1/2} \quad (50)$$

which is similar in form to that obtained earlier by Vessot [19].

For $\omega_1'/\omega_1 \ll \omega_1'\tau \ll 1$,

$$\frac{\sigma(\langle\dot{\phi}\rangle_{t,\tau})}{\omega_0} \approx \left\{\frac{kT}{2P}\left[\frac{F\omega_1'^2 Q_e}{\omega_0^2\tau Q_{c,l}} + \frac{\omega_1'}{2Q_l^2}\right]\right\}^{1/2}. \quad (51)$$

Note that the perturbing noise term in (50) is exactly the same for a maser as that for an ordinary oscillator [see (45)]. For $\tau < F\omega_1' Q_l^2 Q_e/\omega_0^2 Q_{c,l}$ (if $\omega_1'\tau \gg 1$) or $\tau < 2F\omega_1' Q_l^2 Q_e/\omega_0^2 Q_{c,l}$ (if $\omega_1'\tau \ll 1$) the fluctuations due to the additive noise dominate. For a hydrogen maser with $Q_l = 2\times10^9$, $Q_e/Q_{c,l} = 5$, $F = 2$, and $\omega_1' = 60$ the additive noise dominates for $\tau < 30$ seconds. For a rubidium maser with $Q_l = 1\times10^8$ [20] and all other factors the same, the additive noise dominates for $\tau < 6.5\times10^{-3}$ seconds (here $\omega_1'\tau < 1$). Figure 14 is a plot of the theoretical $\sigma(\langle\dot{\phi}\rangle_{t,\tau})/\omega_0$ vs. averaging time for a hydrogen and a rubidium maser. Note again the influence of the narrow filter on the results.

The factors in the two terms of $\sigma(\langle\dot{\phi}\rangle_{t,\tau})/\omega_0$ that depend only on the maser may be collected into figures of merit M_A and M_P, allowing σ to be written as

$$\frac{\sigma(\langle\dot{\phi}\rangle_{t,\tau})}{\omega_0} = \left\{\frac{kT}{2}\left[\frac{F\omega_1'}{M_A^2\tau^2}(1 - e^{-\omega_1'\tau}) + \frac{1}{M_P^2\tau}\left(1 - \frac{(1 - e^{-\omega_1'\tau})}{\omega_1'\tau}\right)\right]\right\}^{1/2} \quad (52)$$

where

$$M_A^2 = \frac{\omega_0^2 P Q_{c,l}}{Q_e} \quad \text{and} \quad M_P^2 = Q_l^2 P.$$

Some typical figures of merit are given in Table I. The figures for quartz assume fairly tight coupling to the load to obtain a large M_A. This is what would be needed

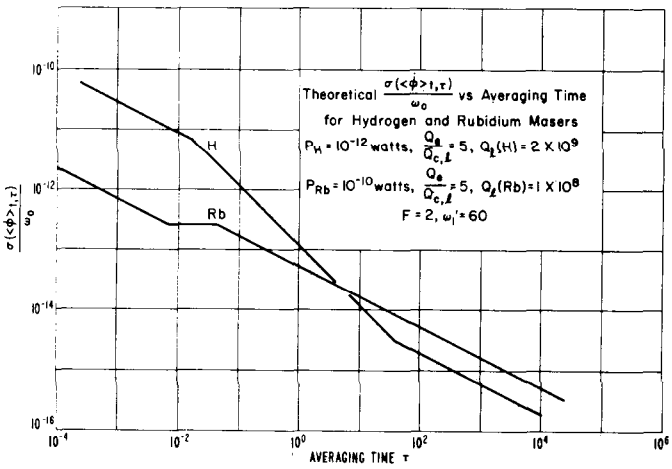

Fig. 14. Theoretical standard deviation of average fractional frequency departure for hydrogen and rubidium masers.

TABLE I

CHARACTERISTICS AND FIGURES OF MERIT OF VARIOUS OSCILLATORS

Type of Oscillator	ω_0—Seconds^{-1}	P—watts	Q_l	$Q_e/Q_{c,l}$	M_P—watts$^{1/2}$	M_A—watts$^{1/2}$ Seconds^{-1}
Ammonia	1.5×10^{10}	1×10^{-10}	5×10^6	5	50	6.7×10^5
Rubidium 87	4.3×10^{10}	1×10^{-10}	1×10^8	5	1000	1.9×10^6
Hydrogen	8.9×10^9	1×10^{-12}	2×10^9	5	2000	4×10^3
Quartz (5 Mc/s)	3.1×10^7	1×10^{-6}	2×10^6	5	2000	1.4×10^4

for an oscillator servoed by a short time constant loop to an atomic device but contrary to the requirements for good long-term stability and freedom from circuit influences in a free running oscillator.

It is very likely that masers also exhibit an f^{-1} power spectral density of frequency fluctuation. This is due to the fact that the frequency is dependent on many external factors that may have an f^{-1} spectral density such as cavity tuning (all masers), magnetic field (hydrogen and rubidium), buffer gas pressure and temperature and light intensity (rubidium), and wall shift (hydrogen). Allan [6] has reported one case where an f^{-1} spectral density was observed for an ammonia maser with some uncertainty in the data. Not many experiments have been performed as yet, partially because of the long times necessary to gather reliable data and also because the field is quite new. This is an interesting area for future research.

V. Fluctuations in Atomic Standards Using a Servo-Controlled Quartz Oscillator

A. Atomic Beam Device

Consider an oscillator compared against a reference such as an atomic beam device [21] and controlled in frequency by a servo actuated by the error signal. Figure 15 shows a system block diagram. The power spectral density of the fluctuations in the output frequency is

$$S_{\dot\phi}(\omega)_0 = S_{\dot\phi}(\omega)_{\mathrm{Osc}} \frac{1}{|1+G(\omega)|^2} + S_{\dot\phi}(\omega)_{\mathrm{Ref}} \left|\frac{G(\omega)}{1+G(\omega)}\right|^2 \quad (53)$$

where $S_{\dot\phi}(\omega)_{\mathrm{Osc}}$ refers to the open loop fluctuations in the oscillator, $S_{\dot\phi}(\omega)_{\mathrm{Ref}}$ refers to the equivalent frequency fluctuations in the reference, and $G(\omega)$ is the total loop gain $K_0K_Rg(\omega)$. In deriving (53) it is assumed that the system is linear and that the two noise sources are uncorrelated. The simplest useful form for $G(\omega)$ (also a very practical one) is

$$G(\omega) = \frac{\omega_c}{j\omega} \quad (54)$$

which is just gain and integration. This is a good approximation to what is done in practice. Substituting, (53) becomes

$$S_{\dot\phi}(\omega)_0 = S_{\dot\phi}(\omega)_{\mathrm{Osc}} \frac{\omega^2}{\omega^2+\omega_c^2} + S_{\dot\phi}(\omega)_{\mathrm{Ref}} \frac{\omega_c^2}{\omega^2+\omega_c^2} \quad (55)$$

so that the oscillator noise is high-pass filtered and the reference noise is low-pass filtered.

Consider first the fluctuations due to the oscillator only. If it is assumed to have characteristics similar to those previously discussed, namely additive noise filtered by a narrow-band filter of half width ω_1, and an f^{-1} behavior, then, if $\omega_1 \gg \omega_c$ (as is usually the case), the additive noise contribution is virtually unchanged by the servo loop. The f^{-1} portion gives, in the closed loop condition, [from (55) and (17a)]

$$\frac{\sigma(\langle\dot\phi\rangle_{t,\tau})}{\omega_0} = \frac{B}{\omega_0\omega_c\tau}\,(1.16 + 2\log\omega_c\tau - e^{-\omega_c\tau}\mathcal{E}i^*(\omega_c\tau) - e^{\omega_c\tau}\mathcal{E}i(-\omega_c\tau))^{1/2} \quad (5$$

where B is a constant depending on the strength of t f^{-1} noise; $\gamma \approx 0.577$ is Euler's constant;

$$\mathcal{E}i(X) = \int_{-\infty}^{X} \frac{e^t}{t}\,dt, \qquad X < 0,$$

is the exponential integral; and $\mathcal{E}i^*(X)$ is the princip value of the integral for $X>0$. This behaves li $(B/\omega_0)[5/2-\gamma-\log(\omega_c\tau)]^{1/2}$ (very slowly varying) f $\omega_c\tau \ll 1$ and like $(B/(\omega_0\omega_c\tau))[2\log(\omega_c\tau)+2\gamma]^{1/2}$ f $\omega_c\tau \gg 1$.

The contribution due to the reference noise, which assumed to be white with power spectral density S_R, [from (55) and (17a)]

$$\frac{\sigma(\langle\dot\phi\rangle_{t,\tau})}{\omega_0} = \frac{1}{\omega_0}\left\{\frac{S_R}{\omega_c\tau^2}(\omega_c\tau + e^{-\omega_c\tau} - 1)\right\}^{1/2}. \quad (5$$

This approaches a constant value of $(1/\omega_0)(S_R\omega_c/2)^{1/2}$ f $\omega_c\tau \ll 1$. For $\omega_c\tau \gg 1$, $\sigma = (1/\omega_0)(S_R/\tau)^{1/2}$ (this holds for ar $G(\omega)$ such that $|G(\omega)/(1+G(\omega))|^2 \to 1$ as $\omega \to 0$ for $\omega \gg 1$). Figure 16 shows the behavior of the various co tributions to the overall fluctuations. It is apparent th there is an optimum choice of loop cutoff ω_c for given oscillator and beam tube.

It is of interest to calculate the power spectral densit

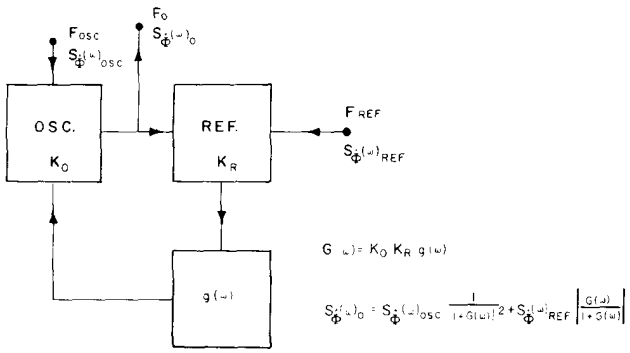

Fig. 15. Block diagram of passive atomic standard.

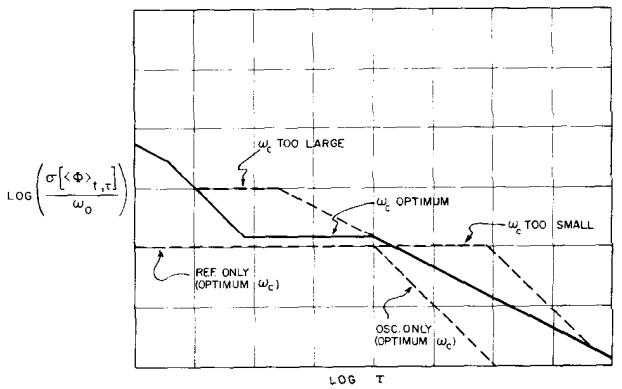

Fig. 16. Contributions to passive atomic standard fluctuations.

of the noise for the case of a cesium beam reference. For Ramsey excitation the response may be written for small departures from line center approximately as

$$I(t) = \frac{I_m}{2}\left\{1 + \cos \pi \left(\frac{\Delta\omega(t)}{\omega_l}\right)\right\} \tag{58}$$

where $I(t)$ is the output current which has a maximum value I_m, $\Delta\omega(t)$ is the departure from line center, and ω_l is the full line width. Let $\Delta\omega(t)/\omega_l = \epsilon + \alpha \cos \omega_m t$ to allow for the usual sinusoidal modulation, where ω_m is the modulation frequency assumed small in comparison with ω_l so that the dynamic behavior is essentially the same as the static behavior. The result of synchronous detection of this signal is

$$I_0 = \frac{I_m \omega_m}{2\pi} \int_{-\pi/\omega_m}^{\pi/\omega_m} \frac{1}{2}(1 + \cos \pi(\epsilon + \alpha \cos \omega_m t)) \cos \omega_m t \, dt$$

$$= -I_m J_1(\pi\alpha) \frac{\sin \pi\epsilon}{2} \approx \frac{-I_m J_1(\pi\alpha)}{2} \epsilon\pi \tag{59}$$

for ϵ small. For a given offset, ϵ, this has the maximum absolute value of $0.91\,\epsilon I_m$ with $\pi\alpha \approx 1.8$, the first maximum of the Bessel function. This represents the signal output for a given fractional mistuning ϵ.

In a beam tube, the noise is mainly due to shot noise and so the power spectral density is proportional to $I(t)^{1/2}$ and is independent of ω. Since $I(t)$ is a function of time, the noise output is not a stationary function. If $i_n(t)$ is the instantaneous noise current with no modulation and $\epsilon = 0$ then

$$I_n(t) = i_n(t)\left|\cos\left(\frac{\pi}{2}\alpha \cos \omega_m t\right)\right|. \tag{60}$$

The autocorrelation function after synchronous detection is desired. Performing the statistical and the time averages gives

$$R_I(\tau) = \delta(\tau)\frac{S_I}{4}(1 + J_0(\pi\alpha) - J_2(\pi\alpha)) \tag{61}$$

where S_I is the spectral density of the noise current. From this and (59) the spectral density S_R is

$$S_R = \frac{S_I|1 + J_0(\pi\alpha) - J_2(\pi\alpha)|\omega_l^2}{J_1^2(\pi\alpha) I_m^2 \pi^2} \tag{62}$$

where S_I is the spectral density of the noise current, I_m is the peak signal current, and $\alpha = (\Delta\omega/\omega_l)_{\max}$ is the ratio of peak frequency swing due to the modulation to the full line width, ω_l. Using these results and assuming optimum modulation amplitude,

$$\frac{\sigma(\langle\dot{\phi}\rangle_{t,\tau})}{\omega_0} = 0.386 \frac{f_l}{f_0} \frac{I_n}{I_m} (\tau)^{-1/2}$$

for averaging time τ long in comparison with the loop time constant, where I_n is the noise current from the beam tube in a 1-c/s noise bandwidth centered about the modulation frequency; $f_l/f_0 = \omega_l/\omega_0$.

B. *Maser with Phase-Locked Oscillator*

Essentially the same sort of analysis that was applied to an oscillator slaved to a passive atomic device may be used for an oscillator phase-locked to a maser. A block diagram of a simple system with the various important noise sources is shown in Fig. 17. Again we have

$$S_{\dot{\phi}}(\omega)_0 = S_{\dot{\phi}}(\omega)_{\text{Osc}} \frac{1}{|1 + G(\omega)|^2} + S_{\dot{\phi}}(\omega)_{\text{Ref}} \left|\frac{G(\omega)}{1 + G(\omega)}\right|^2 \tag{63}$$

where

$$S_{\dot{\phi}}(\omega)_{\text{Ref}} = \frac{S_{\dot{\phi}}(\omega)_{\text{mult}} + S_{\dot{\phi}}(\omega)_m + S_{\dot{\phi}}(\omega)_R + S_{\dot{\phi}}(\omega)_S}{N^2}$$

(see Fig. 17).

As before, the oscillator noise is high-pass filtered and the reference noise is low-pass filtered. Great care must be exercised in the design of the frequency multiplier, receiver, and synthesizer so that their frequency power spectral densities within the loop bandwidth are as small as possible. Solid-state frequency multipliers (and amplifiers) are often plagued with an f^{-1} power spectral density of phase which frequently can be due to f^{-1} noise in biasing or collector voltage supplies. For this type of application temperature control of the frequency multiplier is desirable to remove slow phase drifts with temperature change.

As an example of a possible design, consider locking a relatively high level, tightly coupled 10-Mc/s quartz oscillator to a hydrogen maser. Reasonable estimates for the various pertinent quantities are (hydrogen maser parameters same as in Table I—see also Fig. 17):

$$P_{\text{Osc}} = 10^{-5} \text{ watts},$$

$$\omega_{\text{Osc}} = 6.3 \times 10^7 \text{ second}^{-1},$$

$$N = 140,$$

$$S_{\dot{\phi}}(\omega)_{\text{Osc}} = 10^{-14}\omega^2 + \frac{2 \times 10^{-5}}{|\omega|}, \text{ and}$$

$$S_{\dot{\phi}}(\omega)_{\text{Ref}} = 2 \times 10^{-12}(\omega^2 + 1).$$

It is assumed that the oscillator has an f^{-1}-frequency spectrum plus white phase noise and that the f^{-1} portion leads to a $\sigma(\langle\dot{\phi}\rangle_{t,\tau})/\omega_0 \simeq 10^{-10}$ for $T/\tau \simeq 100$. The reference spectral density is assumed to be due mainly to the additive noise caused by the preamp and mixer (white phase noise) and the random walk term in the maser. The f^{-1} spectral density in the maser is neglected, since presently not much is known about its magnitude (assuming it exists).

In order to reduce the effects of oscillator drift and the f^{-1} spectral density, it is desirable to use a phase-lock loop with two poles at the origin and a zero at ω_2, i.e.,

$$G(\omega) = \frac{2j\omega_2\omega + \omega_2^2}{-\omega^2}.$$

The phase detector provides one pole, and the other

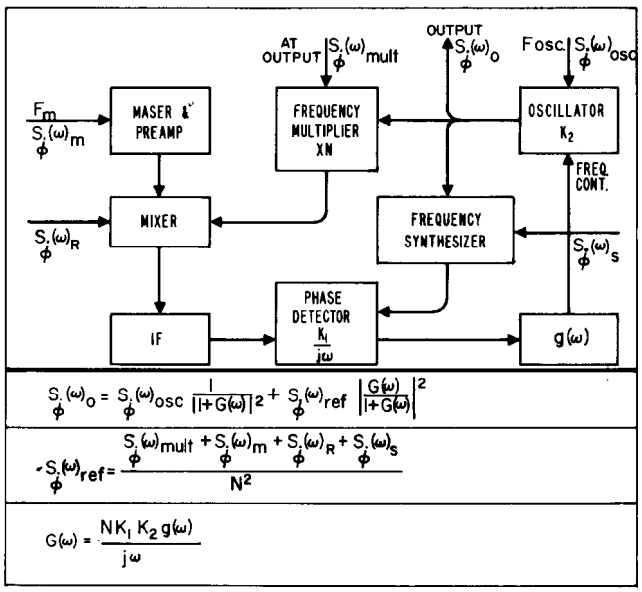

Fig. 17. Block diagram of an active atomic standard with phase-locked quartz oscillator.

pole and the zero may be approximated very well with an operational amplifier with feedback. The loop will be critically damped with this choice of $G(\omega)$, and ω_2 determines the loop cutoff frequency ω_c: i.e., $\omega_c = 2.06\,\omega_2$. With this loop, a constant drift rate in the oscillator produces no frequency error.

The loop cutoff frequency in this example is optimum at the point where the f^{-1} spectral density from the oscillator equals the white phase noise term from the reference. This occurs at $\omega \simeq 215$ seconds^{-1} or $f \simeq 34$ c/s.

The additive noise contribution from the oscillators must be smaller than that from the reference; otherwise, the optimum loop cutoff frequency would be very large. This is the reason for using a fairly high drive level, high-frequency oscillator. Again, careful use of narrow-band filtering of the oscillator can be of great value. Excessive narrow-band filtering may violate servo-stability requirements.

VI. Conclusions

Some of the considerations of the theory and measurement of fluctuations in frequency standards have been presented. It was shown that the fluctuations could be characterized by the autocorrelation function of either frequency or phase or the power spectral density of either frequency or phase. From these the many measures of stability may be computed. Measurement techniques were discussed as well as the techniques for estimating spectral densities, etc. Sources of fluctuations in quartz oscillators, passive atomic standards, and masers were treated and some of the theory presented. In some cases, details have been lightly treated or omitted due to the length of the material presented. It is hoped that the material covered will be useful in promoting understanding and guiding designs.

Appendix I

If $\phi(t)$ is wide-sense stationary and has zero mean

$$\sigma^2(\Delta_\tau\phi(t)) = \overline{(\phi(t+\tau/2) - \phi(t-\tau/2))^2}$$
$$= \overline{\phi(t+\tau/2)^2} - \overline{2\phi(t+\tau/2)\phi(t-\tau/2)} + \overline{\phi(t-\tau/2)^2} = 2(R_\phi(0) - R_\phi(\tau)) \quad (64)$$

which leads to (16a) in the text, since $\sigma^2(\langle\dot\phi\rangle_{t,\tau}) = (1/\tau^2)\sigma^2(\Delta_\tau\phi(\tau))$.

$$\sigma^2(\langle\dot\phi\rangle_{t,\tau}) = \frac{1}{\tau^2}\int_{-\tau/2}^{\tau/2} dt' \int_{-\tau/2}^{\tau/2} dt''\, \overline{\dot\phi(t')\dot\phi(t'')}$$
$$= \frac{1}{\tau^2}\int_{-\tau/2}^{\tau/2} dt' \int_{-\tau/2}^{\tau/2} dt'' R_{\dot\phi}(t''-t'). \quad (65)$$

Let $(t''-t')=\tau'$. Using this substitution and interchanging the order of integration gives

$$\sigma^2(\langle\dot\phi\rangle_{t,\tau}) = \frac{2}{\tau}\int_0^\tau R_{\dot\phi}(\tau')\left(1-\frac{\tau'}{\tau}\right)d\tau' \quad (66)$$

which gives (16b).

The second phase difference $\Delta_\tau^2\phi(t)$ is $[\phi(t+\tau)-\phi(t)] - [\phi(t)-\phi(t-\tau)]$ or $\phi(t+\tau)-2\phi(t)+\phi(t-\tau)$.

$$\sigma^2(\Delta_\tau^2\phi(t)) = \overline{(\phi(t+\tau) - 2\phi(t) + \phi(t-\tau))^2}$$
$$= 6R_\phi(0) - 8R_\phi(\tau) + 2R_\phi(2\tau) \quad (67)$$

leading to (46).

Appendix II

Assume that a signal $v(t)$ is observed for a time T, and it is desired to remove the mean and the linear drift in a least square departure sense. This requires that

$$\int_{T/2}^{T/2} (v(t) - (a+bt))^2\, dt = \text{minimum}. \quad (68)$$

For this to be satisfied

$$a = \frac{1}{T}\int_{-T/2}^{T/2} v(t)\, dt,$$
$$b = \frac{12}{T^3}\int_{-T/2}^{T/2} tv(t)\, dt. \quad (69)$$

Consider the Fourier transform of

$$v'(t) = v(t) - (a+bt), \qquad |t| < T/2$$
$$= 0, \qquad |t| > T/2$$
$$V'(\omega) = \int_{-T/2}^{T/2} v'(t)e^{-j\omega t}\, dt. \quad (70)$$

Expanding the kernel gives an approximation to $V'(\omega)$ for $\omega T/2 < 1$:

$$V'(\omega) = \int_{-T/2}^{T/2} v'(t)\left(1 - j\omega t - \frac{\omega^2t^2}{2} + \cdots\right)dt$$
$$= \int_{-T/2}^{T/2} (v(t) - a - bt)\left(1 - j\omega t - \frac{\omega^2t^2}{2} + \cdots\right)dt. \quad (71)$$

If the integrals that can be done are carried out and the values of a and b substituted, it will be seen that $V'(\omega)$ has neither a constant term nor a term linear in ω. Also the transform of $a+bt$ goes to zero rapidly for $\omega \gg 2/T$. Thus, sampling for time T and removing the mean and the linear drift is quite similar to passing $v(t)$ through a high-pass filter with two zeros, cutting off at about $\omega = 2/T$. Another way to show this is to consider the minimization of

$$\frac{1}{2\pi}\int_{-\infty}^{\infty} |\, V'(\omega)\,|^2\, d\omega = \int_{-T/2}^{T/2} (v'(t))^2\, dt \qquad (72)$$

the equality holding because of Parseval's Theorem. Adjusting the parameters a and b for minimum total energy is really removing the maximum amount of energy possible in the band of frequencies occupied by the transform of $a+bt$. Since this transform has a half width of the order of $2/T$, the whole process is quite similar to the high-pass filter mentioned earlier. Subtracting a second-order and third-order term in t would about double the cutoff frequency.

We may obtain the corresponding general result for subtraction of an Nth order polynomial, $g_N(t)$, from $v(t)$. For

$$\int_{-T/2}^{T/2} (v(t) - g_N(t))^2 dt$$

to be a minimum we may let

$$g_N(t) = \sum_{n=0}^{N} a_n P_n(2t/T)$$

where $P_n(x)$ is the Legendre polynomial of the first kind and a_n is a constant to be determined. ($N=1$ is the linear regression case considered earlier.) This follows from the mean square approximation property of orthonormal sets of functions: $P_n(2t/T)$ is the orthonormal set of polynomials for the interval $|t| < T/2$ with weight function unity. In the usual way we find

$$a_n = \frac{2n+1}{T}\int_{-T/2}^{T/2} v(t) P_n(2t/T)dt$$
$$= \frac{2n+1}{T}\int_{-\infty}^{\infty} \hat{v}(t) P_n(2t/T)dt$$

where $\hat{v}(t) = v(t)$ for $|t| < T/2$ and $\hat{v}(t) = 0$ for $|t| > T/2$.

Consider the Fourier transform, $\hat{G}_N(w)$, of $\hat{g}_N(t)$ where $\hat{g}_N(t) = g_N(t)$ for $|t| < T/2$ and $\hat{g}_N(t) = 0$ for $|t| > T/2$.

$$\hat{G}_N(w) = \int_{-\infty}^{\infty} \hat{g}(t) e^{-j\omega t} dt$$
$$= \sum_{n=0}^{N} a_n \int_{-T/2}^{T/2} P_n(2t/T) e^{-j\omega t} dt$$
$$= T \sum_{n=0}^{N} a_n (-j)^n j_n(wT/2)$$

where $j_n(x)$ is the spherical Bessel function of the first kind. We may express the coefficient a_n in terms of $\hat{V}(w)$, the Fourier transform of $\hat{v}(t)$:

$$a_n = \frac{2n+1}{T}\int_{-\infty}^{\infty} \hat{v}(t) P_n(2t/T)dt$$
$$= \frac{2n+1}{T}\left[P_n\left((2j/T)\left(\frac{d}{dw}\right)\right)\hat{V}(w)\right]\Big|_{w=0}$$

where d/dw is the differential operator and the expression is evaluated at $w=0$ after the differentiations are performed. We find, using the expansions for the Bessel functions, that as

$$WT/2 \to 0$$
$$\hat{G}_0(w) \to \hat{V}(0),$$
$$\hat{G}_1(w) \to \hat{V}(0) + w\hat{V}'(0),$$
$$\hat{G}_2(w) \to \hat{V}(0) + w\hat{V}'(0) + \frac{w^2}{2}\left(\hat{V}''(0) + \frac{\hat{V}(0)T_2}{12}\right),$$
$$\left(\hat{V}'(0) = \left[\frac{d}{dw}\hat{V}(w)\right]\Big|_{w=0}\right)$$

and for $wT/2 \gg 1$, $\hat{G}_N(w) = 0$. Thus, if $\hat{g}_0(t)$ (the average value of $\hat{v}(t)$ is subtracted from $\hat{v}(t)$, the transform of the difference has a single zero at $w=0$, and subtraction of $\hat{g}_1(t)$ (linear regression) gives two zeros. Note that subtraction of higher order terms such as $\hat{g}_2(t)$ does not introduce more zeros. Also, since $\hat{G}_N(w) \to 0$ for $wT/2 \gg 1$, the transform of $\hat{v}(t) - \hat{g}_N(t)$ is just $\hat{V}(w)$ for large $WT/2$. This again demonstrates the high-pass filtering action.

The next consideration is to calculate the average of the estimates of the variance for a signal $v(t)$ observed for only a finite time T. It is assumed that $v(t)$ represents a stationary ergodic process and has zero mean. The variance is

$$\sigma^2(v) = \overline{v(t)^2} = \langle v^2 \rangle = R_v(0) = \frac{1}{2\pi}\int_{-\infty}^{\infty} S_v(\omega)\, d\omega. \qquad (73)$$

The estimate of the variance over time T is

$$\hat{\sigma}^2(v) = \langle v^2 \rangle_{t,T} - \langle v \rangle_{t,T}^2$$
$$= \frac{1}{T}\int_{t-T/2}^{t+T/2} v^2(t')\, dt' - \frac{1}{T^2}\left(\int_{t-T/2}^{t+T/2} v(t')\, dt'\right)^2. \qquad (74)$$

The average value of the estimate variance is

$$\bar{\hat{\sigma}}^2(v) = \frac{1}{T}\int_{t-T/2}^{t+T/2} \overline{v^2(t')}\, dt'$$
$$- \frac{1}{T^2}\int_{t-T/2}^{t+T/2} dt' \int_{t-T/2}^{t+T/2} dt'' \overline{(v(t')v(t''))}$$
$$= \sigma^2(v) - \frac{1}{T^2}\int_{t-T/2}^{t+T/2} dt' \int_{t-T/2}^{t+T/2} dt'' R_v(t'' - t')$$
$$= \frac{1}{2\pi}\int_{-\infty}^{\infty} d\omega S_v(\omega)\left(1 - \frac{\sin^2 \omega T/2}{(\omega T/2)^2}\right). \qquad (75)$$

(The bar here means either statistical or time average.) Thus, the average of the estimated variance is the same as the true variance except for the factor

$$\left(1 - \frac{\sin^2 \omega T/2}{(\omega T/2)^2}\right)$$

in the integrand. For $\omega T/2 \ll 1$, this factor is approximately $1/3$ $(\omega T/2)^2$ and for $\omega T/2 \gg 1$, the factor goes to 1. Here again is the high-pass filtering action, the filter cutting off at $\omega \simeq 2/T$.

If $v(t)$ is taken to be

$$\langle \dot{\phi} \rangle_{t,\tau} = \frac{1}{\tau} \int_{t-\tau/2}^{t+\tau/2} \dot{\phi}(t')dt' = \frac{\Delta_\tau \phi(t)}{\tau}$$

corresponding to *averaging* the frequency over time τ and *observing* it for time T,

$$\overline{\hat{\sigma}^2(\langle \dot{\phi} \rangle_{t,\tau})} = \frac{1}{2\pi} \int_{-\infty}^{\infty} S_{\dot{\phi}}(\omega) \left(\frac{\sin^2 \omega\tau/2}{(\omega\tau/2)^2}\right) \cdot 1 - \frac{\sin^2 \omega(T-\tau)/2}{(\omega(T-\tau)/2)^2} d\omega, \tag{76}$$

since

$$S_{\langle \dot{\phi} \rangle_{t,\tau}}(\omega) = S_{\dot{\phi}}(\omega) \frac{\sin^2 \omega\tau/2}{(\omega\tau/2)^2}$$

which may be shown either by direct calculation of the Fourier transform of the autocorrelation function of

$$\langle \dot{\phi} \rangle_{t,\tau} = (\phi[t+(\tau/2)] - \phi[t-(\tau/2)])/\tau$$

and using the relation $S_{\dot{\phi}}(\omega) = S_\phi(\omega)/\omega^2$ or by the method used in the text following (22). $T-\tau$ appears in place of T in (76), since only $T-\tau$ is available for averaging. Note that since the factor

$$[1 - \sin^2 \omega(T-\tau)/2/(\omega(T-\tau)/2)^2]$$

goes to zero as ω^2, the integral will be convergent for an f^{-1} behavior of $S_{\dot{\phi}}(\omega)$. If $\langle \dot{\phi} \rangle_{t,\tau}$ is taken to be a discrete variable (as is usually done in the actual measurements) the average of the estimated variance will be [6], [14]

$$\overline{\hat{\sigma}^2_{N,\langle \dot{\phi} \rangle_{t,\tau}}} = \frac{1}{2\pi} \int_{-\infty}^{\infty} S_{\dot{\phi}}(\omega) \frac{\sin^2 \omega\tau/2}{(\omega\tau/2)^2} - \frac{\sin^2 N\omega\tau/2}{(N\omega\tau/2)^2} d\omega \tag{77}$$

which is very similar to (76). Here, instead of using a continuous average over T to compute σ, the average is over N discrete consecutive samples of $\langle \dot{\phi} \rangle_{t,\tau}$ each spaced time τ apart so that $N\tau$ corresponds to T in the continuous case. For a detailed discussion of the discrete variable formulation see Allan [6] and Barnes [14].

The bar over $\hat{\sigma}^2$ in (75), (76), etc. implies averaging over a number of periods of time of length $(T-\tau)$ to obtain the average of $\hat{\sigma}^2$. This is necessary since $\hat{\sigma}$ is really a statistical variable and has its own variance [1].

Usually $T \gg \tau$ in (76) and the spectral density will be fairly smooth so that if (76) converges the high-pass filter action may be approximated by a low-frequency cutoff on the integral. Thus

$$\overline{\hat{\sigma}(\langle \dot{\phi} \rangle_{t,\tau})} \approx \frac{1}{\pi} \int_{2/T}^{\infty} S_{\dot{\phi}}(\omega) \left| \frac{\sin^2 \frac{\omega\tau}{2}}{\left(\frac{\omega\tau}{2}\right)^2} \right| d\omega. \tag{78}$$

Let us now calculate the fluctuation expected in a finite time of observation of an oscillator with an f^{-1} power spectral density of frequency. Assume

$$S_{\dot{\phi}}(\omega) = \frac{K}{|\omega|}$$

so that

$$S_\phi(\omega) = \frac{K}{|\omega|^3}.$$

If the oscillator were observed for an infinite time

$$\sigma^2(\Delta_\tau \phi(t)) = 2(R_\phi(0) - R_\phi(\tau)) = \frac{2K}{\pi} \int_0^{\infty} \frac{1 - \cos \omega\tau}{\omega^3} d\omega$$

which of course does not converge. If we cut off the integral at the lower limit $2/T$ corresponding to (78)

$$\sigma^2 = \frac{2K}{\pi} \int_{2/T}^{\infty} \frac{1 - \cos \omega\tau}{\omega^3} d\omega = \frac{2K\tau^2}{\pi} \int_{2\tau/T}^{\infty} \frac{1 - \cos x}{x^3} dx.$$

For constant T/τ the integral is a constant and $\sigma^2 = C^2\tau^2$, C a constant. Then, we have

$$\frac{\sigma(\langle \dot{\phi} \rangle_{t,\tau})}{\omega_0} = \frac{1}{\omega_0 \tau} \sigma(\Delta_\tau \phi(t)) = \text{constant}.$$

To get the dependence on T/τ we can estimate the integration. (The integral can be done exactly in terms of the cosine integral.)

$$\frac{\sigma^2(\langle \dot{\phi} \rangle_{t,\tau})}{\omega_0^2} = \frac{2K}{\pi\omega_0^2} \int_{2\tau/T}^{\infty} \frac{1 - \cos x}{x^3} dx = \frac{2K}{\pi\omega_0^2} \cdot \left(1.04 + \frac{1}{2} \log\left(\frac{T}{2\tau}\right) + O\left(\left(\frac{2\tau}{T}\right)^2\right)\right).$$

So for $T/2\tau \gg 1$ $\sigma^2(\langle \dot{\phi} \rangle_{t,\tau})/\omega_0^2$ is proportional to $\log (T/2\tau)$.

The problem of spectral density estimation from data over a finite time is well covered in the literature [1], [22]. For the relatively high-frequency portions, say $\omega > 20$, analysis of the signal representing $\phi(t)$ or $\dot{\phi}(t)$ by the usual narrow-band and tunable filter is simple and useful if the resolution required is not too great. The techniques of carrier cancellation and sideband exaltation by using a dispersive bridge or a nondispersive delay line are also extremely useful [23], [24].[3]

[3] Several papers and correspondence items in this issue contain material pertaining to these types of measurements.

For lower frequencies it is usually necessary to do the spectral analysis from the time data. One technique is to compute an approximate autocorrelation function, modify it with a time window (Hanning, Hamming, or other [1]), $D(\tau)$, which is symmetric about $\tau=0$, equals 1 for $\tau=0$, and goes smoothly to zero and then stays zero for some $\tau \leq T$, where T is the total time duration of the data. Then the Fourier transform of this modified autocorrelation function is computed to get the estimate of the spectral density. One can then show that if $\hat{S}(\omega)$ is an estimate of the spectral density computed in this way then $\bar{\hat{S}}(\omega)=S(\omega)\otimes Q(\omega)$ where $S(\omega)$ is the true spectral density, $\otimes$ signifies convolution, the bar signifies the statistical average, and $Q(\omega)$ is the Fourier transform of the time window. The variance of $\hat{S}(\omega)$ depends on the shape of the time window as well as the ratio of the length (in time) of the time window to the total length in time of the data. For small ratios the variance is small, but the smearing of the spectrum due to the consequently wide $Q(\omega)$ is appreciable. For any given length of data, therefore, there is some variance and some smearing. The time window represented by (24) is

$$D_c(\tau) = 1 - \frac{|\tau|}{T}, \quad |\tau| \leq T; \qquad D_c(\tau) = 0, \quad |\tau| > T.$$

Since this time window is as wide as is possible from the data length, the variance of $\hat{S}(\omega)$ will be fairly large. As pointed out in Blackman and Tukey [1], it is wise to remove the mean and the linear drift before attempting spectral analysis via the autocorrelation function route.

Low-frequency analysis can also be done by observing the slope of $\sigma(\langle\phi\rangle_{t,\tau})/\omega_0$, or by successive differences of phase [14], or by observing

$$\sigma^2(\phi'(\omega))_{\omega_c} = \frac{1}{2\pi}\int_{-\infty}^{\infty} S_\phi(\omega)\,|\,H(\omega,\,\omega_c)\,|^2 d\omega$$

as a function of the cutoff frequency ω_c of a low-pass filter $H(\omega, \omega_c)$ through which the signal representing $S_\phi(\omega)$ is passed [25].

Acknowledgment

The authors would like to thank R. Vessot of Varian Associates, Beverly, Mass., J. Barnes of NBS, Boulder, Colo., and J. W. Graham, R. P. Rafuse, and J. G. King at M.I.T., Cambridge, Mass., for helpful discussions; also, L. Bodily and A. Foster of the Hewlett-Packard Co., Palo Alto, Calif., R. S. Badessa of M.I.T., and R. D. Posner, formerly of M.I.T., now with Aeronutronics, Newport Beach, Calif., for making some of the measurements.

References

[1] R. B. Blackman and J. W. Tukey, *The Measurement of Power Spectra*. New York: Dover, 1959.
[2] W. B. Davenport and W. L. Root, *Random Signals and Noise*. New York: McGraw-Hill, 1958, ch. 6.
[3] *Ibid.*, ch. 4, sec. 4.5.
[4] C. L. Searle and D. A. Brown, "Comparison of performance criteria of frequency standards," *Proc. 1962 16th Annual Symp. on Frequency Control*, pp. 259–266.
[5] J. Rarity, L. Saporta, and G. Weiss, "Study of short term stability of crystal oscillators," New York University, New York, N. Y., Tech. Rept., Contract DA-36-039-SE-87450, DA Project 3A-99-15-02, -02-02.
[6] D. W. Allan, "Statistics of atomic frequency standards," this issue, page 221.
[7] R. Vessot, L. Mueller, and J. Vanier, "The specification of oscillator characteristics from measurements made in the frequency domain," this issue, page 199. See also Vessot et al., "A cross-correlation technique for measuring the short-term properties of stable oscillators," *IEEE-NASA Symp. on Short-Term Frequency Stability*, Washington, D. C.: U. S. Govt. Printing Office, pp. 111–118, NASA SP-80.
[8] V. Van Duzer, "Short term stability measurements," *ibid.*, pp. 269–272, and private communication.
[9] R. D. Posner, "Digital computer aided calculation of frequency stability," M.S. thesis, M.I.T., Cambridge, Mass., June 1965.
[10] W. R. Atkinson, L. Fey, and J. Newman, "Spectrum analysis of extremely low frequency variations of quartz oscillators," *Proc. IEEE (Correspondence)*, vol. 51, p. 379, February 1963.
[11] D. Hammond, C. Adams, and L. Cutler, "Precision crystal units," *Proc. 1963 17th Annual Symp. on Frequency Control.*
[12] A. W. Warner, "Design and performance of ultraprecise 2.5 mc quartz crystal units," *Bell Sys. Tech. J.*, vol. 39, p. 1193, September 1960.
[13] W. A. Edson, "Noise in oscillators," *Proc. IRE*, vol. 48, pp. 1454–1466, August 1960. See also J. A. Mullen, "Background noise in oscillators," and M. Golay, "Monochromaticity and noise in a regenerative electrical oscillator" in the same issue.
[14] J. A. Barnes, private communication, and J. A. Barnes and D. W. Allan, "Effects of long term stability on the definition and measurement of short term stability," *Proc. 1964 Symp. on Definition and Measurement of Short-Term Frequency Stability.* Also, J. A. Barnes, "Atomic timekeeping and the statistics of precision signal generators," this issue, page 207.
[15] D. Kleppner, H. Goldenberg, and N. F. Ramsey, *Phys. Rev.*, vol. 126, p. 603, 1962.
[16] K. Shimoda, T. Wang, and C. H. Townes, *Phys. Rev.*, vol. 192, p. 1308, 1956.
[17] L. Cutler, to be published.
[18] E. Hafner, "The effects of noise in oscillators," this issue, page 179.
[19] R. F. C. Vessot and H. Peters, "Frequency beat experiments with hydrogen masers," *Proc. 1963 17th Annual Symp. on Frequency Control.*
[20] P. Davidovits and R. Novick, "The optically pumped rudidium maser," this issue, page 155.
[21] J. J. Bagnall, Jr., "The effect of noise on an oscillator controlled by a primary reference," *NEREM 1959 Record*, pp. 84–86.
[22] W. B. Davenport and W. L. Root [2], sec. 6-6.
[23] I. Berstein and G. Gorelik, "Frequency modulation noise in oscillators," *Proc. IRE (Correspondence)*, vol. 45, p. 94, January 1957.
[24] I. Berstein, "On the fluctuations of a vacuum tube oscillator," *Reports of the Academy of Science, USSR*, vol. 68, no. 3, pp. 469–472, 1949.
[25] R. F. C. Vessot, private communication. See also Vessot et al. [7].
[26] E. J. Baghdady, R. N. Lincoln, and B. D. Nelin, "Short term frequency stability characterization, theory, and measurement"; L. S. Cutler, "Some aspects of the theory and measurement of frequency fluctuations in frequency standards;" V. J. Bates, R. S. Badessa, R. D. Posner, and C. L. Searle, "Computer-aided calculation of frequency stability," all in *Proc. IEEE-NASA Symp. on Short Term Frequency Stability*. Washington D. C.: U. S. Govt. Printing Office, 1964, NASA SP-80, no. 20402. Baghdady et al. also appears in *Proc. IEEE*, vol. 53, pp. 704–722, July 1965.
[27] S. L. Johnson, B. H. Smith, and D. A. Calder, "Noise spectrum characteristics of low-noise microwave tubes and solid-state devices," this issue, page 258.